European Journal of Medicinal Chemistry 138 (2017) 328–342

Contents lists available at ScienceDirect

European Journal of Medicinal Chemistry

journal homepage: http://www.elsevier.com/locate/ejmech

Research paper

Leucine rich repeat kinase 2 (LRRK2) inhibitors based on indolinone scaffold: Potential pro-neurogenic agents

Irene G. Salado [a, 1], Josefa Zaldivar-Diez [a, 1], Victor Sebastian [a], Lingling Li [b], Larissa Geiger [a], Silvia González [a], Nuria E. Campillo [a], Carmen Gil [a], Aixa V. Morales [b], Daniel I. Perez [a, **], Ana Martinez [a, *]

[a] Department of Chemical and Physical Biology, Centro de Investigaciones Biológicas-CSIC, Madrid, Spain
[b] Department of Molecular, Cellular and Developmental Neurobiology, Instituto Cajal-CSIC, Madrid, Spain

ARTICLE INFO

Article history:
Received 4 May 2017
Received in revised form
27 June 2017
Accepted 28 June 2017
Available online 29 June 2017

Keywords:
LRRK2 inhibitors
Protein kinase inhibitors
Indolinone
Adult neurogenesis
Neural stem cell
Regenerative medicine

ABSTRACT

Leucine-rich repeat kinase 2 (LRRK2) is one of the most pursued targets for Parkinson's disease (PD) therapy. Moreover, it has recently described its role in regulating Wnt signaling and thus, it may be involved in adult neurogenesis. This new hypothesis could give rise to double disease-modifying agents firstly by the benefits of inhibiting LRRK2 and secondly by promoting adult neurogenesis. Herein we report, the design, synthesis, biological evaluation, SAR and potential binding mode of indoline-like LRRK2 inhibitors and their preliminary neurogenic effect in neural precursor cells isolated from adult mice ventricular-subventricular zone. These results open new therapeutic horizons for the use of LRRK2 inhibitors as neuroregenerative agents. Moreover, the indolinone derivatives here prepared, inhibitors of the kinase activity of LRRK2, may be considered as pharmacological probes to study the potential neuroregeneration of the damaged brain.

1. Introduction

The search of effective treatments for neurodegenerative diseases is one of the urgent clinical and social needs today given their widespread and devastating nature. As most neurodegenerative disorders are age-dependent, due to longer life expectancy the prevalence of these diseases, including Alzheimer's and Parkinson's disease among others, increases daily. Common characteristics of neurodegenerative diseases include the progressive loss of neurons in specific regions of the nervous system underlying the subsequent decline in cognitive or motor function in patients. Given their largely unknown etiology and the lack of effective treatments there is a critical need to better understand the underlying disease pathophysiology and discover effective disease-modifying targets for their treatment.

Genetic studies carried on several families in Asia, the United States, and Europe led to discover in 2004 that mutations in the gene *LRRK2* encoding leucine-rich repeat kinase 2 (LRRK2) as a major genetic risk factor for both familial and sporadic Parkinson's disease (PD) [1]. Up to date among the disease-linked genetic polymorphisms (15% of the total PD population) LRRK2 mutations account for 4% of the cases and 1% of the sporadic ones [2]. Although these incidences are quite low and it remains unclear how mutations in *LRRK2* gene cause PD-related neurodegeneration, LRRK2 has raised as one of the most pursued targets for PD and its inhibition has been proposed to be beneficial for preventing neurodegeneration. Big efforts are being done at the moment both from academia and the pharmaceutical industry with the goal of developing selective and brain-permeable LRRK2 inhibitors as neuroprotective agents for PD [3,4].

LRRK2 is an unusually large (2527 amino acids) protein that is classified as a member of the Ras-like GTPase (ROCO) superfamily. At least 6 independent domains have been established including a kinase domain, a GTPase domain and several protein-protein interacting regions [5]. The physiological role of LRRK2 is poorly understood and many of its substrates remain unclear, however, great success was achieved by the identification of a subset of Rab GTPases as key LRRK2 substrates [6]. The downstream signals in

* Corresponding author.
** Corresponding author.
E-mail addresses: dperez@cib.csic.es (D.I. Perez), ana.martinez@csic.es (A. Martinez).
[1] Equally contributed to this work.

http://dx.doi.org/10.1016/j.ejmech.2017.06.060
0223-5234/

which LRRK2 is involved are not well characterized yet, however LRRK2 can be related to other pathological pathways outside the direct PD pathology. LRRK2 can be related to tau pathology, inflammatory response, oxidative stress, mitochondrial and synaptic dysfunction, deficiencies in the autophagy-lysosomal system [7] and its implication in adult neurogenesis through the Wnt signaling pathway [8].

Among these connections we considered as the most interesting one, the hypothesis that the pharmacological inhibition of LRRK2 may induce adult neurogenesis. There is evidence suggesting that neurogenesis is impaired in many neurodegenerative diseases, therapeutic approaches that stimulate neurogenesis may have potential to stimulate repair and even recovery, thereby providing innovative, disease-modifying treatments [9,10]. Therefore, LRRK2 inhibitors may have a dual therapeutic role: the first one due to the direct beneficial effect of LRRK2 inhibition and the second one as enhancing adult neurogenesis.

Based on these collective observations pointing to the critical role of LRRK2 in CNS function and connections to proneurogenic pathways like Wnt signaling [8], we initiated a medicinal chemistry program with the aim of finding new selective LRRK2 inhibitors with physicochemical properties compatible with crossing the blood brain barrier (BBB). Furthermore, we have used them as pharmacological probes of adult neurogenesis activators using neural stem cells isolated from the neurogenic niche of the adult mouse ventricular-subventricular zone [11]. In this communication we present a class of outstanding novel LRRK2 inhibitors that show a preliminary effect in increasing the proliferation of neural stem cells from the subventricular zone of adult mice and can therefore be considered as chemical probes to study the neuroregeneration potential of the damaged brain.

2. Results and discussion

2.1. Design of new compounds

Biology-oriented synthesis [12] employs chemical privileged scaffolds from natural sources for the development of focused libraries because natural products are particularly important as source of inspiration for new compounds [13]. A literature survey identified several isatin (1*H*-indole-2,3-dione) derivatives as, a natural scaffold present in different Chinese traditional medicines, with potent biological activity on different protein kinases (Fig. 1) [14]. Moreover, some of them such as sunitinib are FDA approved for human therapy while semaxanib is currently in clinical trials (Fig. 1) [15].

For the design of new LRRK2 inhibitors, we decided to keep the indolinone ring as common and privileged scaffold and to modify the nature of the atom directly joined to the oxindole ring introducing a nitrogen atom instead of the carbon atom present in the compounds of Fig. 1. Furthermore, the influence of various substituents on the aryl group was explored obtaining different compounds, with aromatic and aliphatic nature. In addition, the linker between the above mentioned substituent and the oxoindole heterocycle was modified. Imines and hydrazones were used for this purpose. Finally, alkylation of the heterocyclic nitrogen atom and substitution in different positions of the indolinone framework gave additional diversity to the final compounds (Fig. 2).

2.2. Chemistry

Preparation of the first family of these compounds was carried out using classical conditions to conduct the imine formation reaction between the isatin core and the corresponding aromatic amine under reflux in toluene and with 4-toluensulfonic acid as catalyst [16]. Several imino indolinone derivatives have been previously described. However, due to long reaction times and low yields, new synthetic reaction conditions were looked for. Microwave assisted organic synthesis in the absence of solvent and montmorillonite (MMT-K10) as surface catalyst were the best option found [17], although here an optimized work-up was used (described in the experimental part). MMT-K10 is a mixture of silicates in laminar arrangement recently used as inorganic base in organic synthesis. The reactions catalysed by MMT-K10 are normally performed under mild conditions to obtain high yield and selectivity. MMT-K10 was not only used as a base but also as a solid surface where the reaction took place [18]. For imine formation it is essential to remove the water from the reaction medium and normally 4-toluenesulfonic acid was used. In our case, the use of microwave assisted organic synthesis accelerates the dehydration of the reaction using a clay support MMT-K10. Thus, lower reaction times (10 min) and an increase in general yield was achieved except

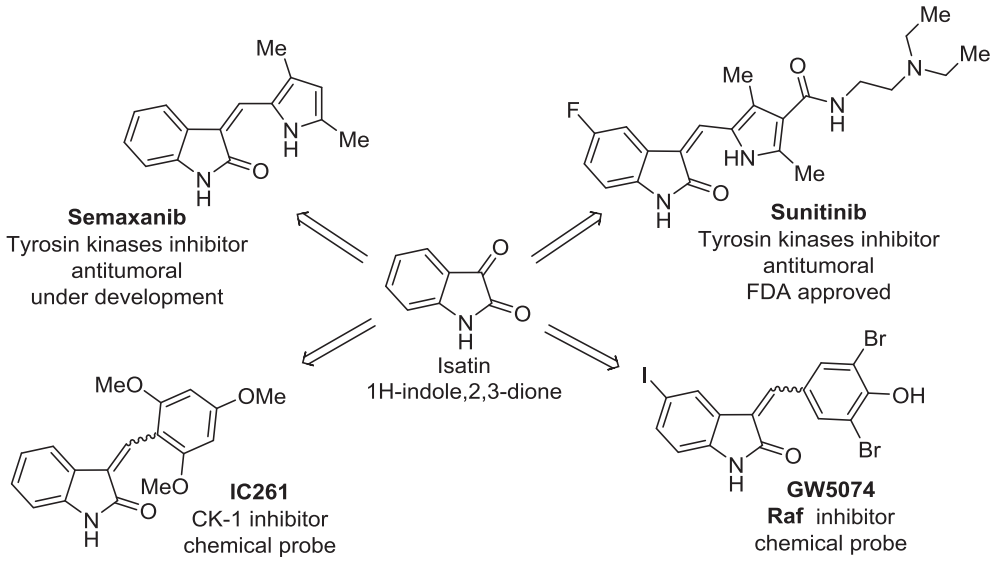

Fig. 1. Structure of known protein kinase inhibitors with indolinone scaffold.

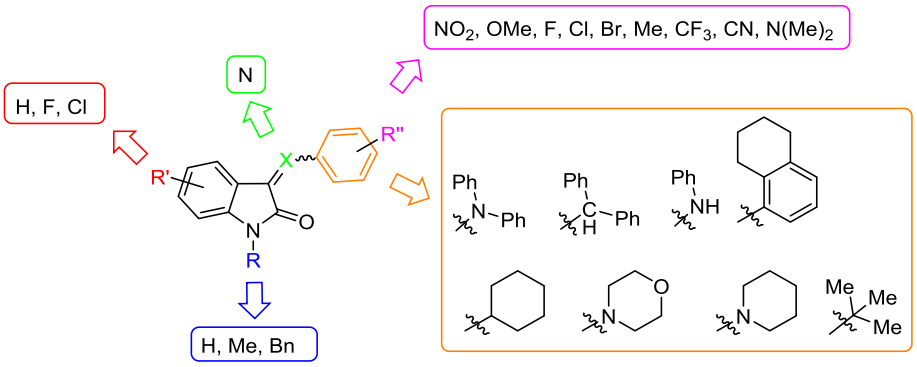

Fig. 2. Designed compounds following a biology-oriented synthesis (BIOS) approach and consideration of the indolinone ring as a privileged scaffold.

for compounds **7** and **9** where the amine employed was in the hydrochloride form. Following this optimized procedure, compounds **1**–**15** were isolated (Scheme 1).

The second family of compounds bears in their chemical structure aliphatic cyclic scaffolds as piperidine, morpholine or diphenylhydrazine among others (**16**–**21**) instead of a phenyl ring. This involves a change in the nature of the linker to the isatin core from an imino to a hydrazone one (Scheme 1).

In order to explore the importance of the nitrogen atom of the isatin derivative, we *N*-alkylated the previously synthetized compounds employing classical conditions [19] which led us to derivatives **22**–**27**. Nevertheless, in the case of imine derivatives, acidic medium leads to the hydrolysis of the imine bond. For this reason, the *N*-alkylation of the isatin heterocycle was done previously to the imine formation leading to compounds **28**–**29**. Further reactions with different anilines yielded the desired compounds **30**–**32** (Scheme 1).

Finally, to introduce an alternative diversity point, the isatin core with different substituents in positions 5 and 7 were used as starting materials leading to the final products **33**–**50**.

All the synthesized compounds were carefully characterized by mass spectra (MS), ^{1}H and ^{13}C-NMR including bidimensional HMBC and HSQC experiments, and when possible for some previously described compounds, melting points were compared (see experimental). Elemental analysis was performed for all the new herein reported compounds (see supporting information Table S1).

The indolinones with imino or hydrazone bond directly attached to the heterocyclic framework may present two different isomers *E* and *Z* that were identified and quantified by ^{1}H-NMR (Table 1). In order to determine the main isomer, a nuclear Overhauser effect (nOe) experiment was carried out. Thus, by irradiation performed in the indolinone H4 proton, a nOe effect of the aromatic protons of the phenyl ring is observed for the *E*-isomer, while it is not detected for the *Z*-isomer (Fig. 3). This methodology was carried out in all the cases to determine the isomers ratio of the compounds. For the first family of synthesized compounds, the oxoindole iminoderivatives **1**–**15** and **30**–**32,** the main isomer obtained was the *E* form although the *Z* one was also detected. Differences observed in the isomers ratio could be justify by the electron donor or electron acceptor substituents present on the phenyl ring. However for compounds **17** and **18**, the main isomer was found to be the *Z* one. In these compounds an intramolecular hydrogen bond could be formed between the carbonyl group of the indolinone core and the CH or NH of the imino or hydrazine bond, respectively.

In compounds where the hydrazone linker was present (derivatives **16**, **19**–**27**, **33**–**38**), nOe experiments revealed that the main and in some cases such as compounds **37** and **38**, the only isomer obtained was the *E* one due to the hydrogen bond formation between the H4 proton of the indolinone core and the nitrogen atom of the hydrazone moiety. If any substituents are present in the indolinone heterocycle, their piperidine (**39**–**43**) or morpholine (**44**–**50**) derivatives lead to obtain the *Z* isomer as the majority. However, when there is no substitution in the oxoindole core, both isomers *E* and *Z* are found in the same ratios (see compounds **19**, **24**, **26**, **27**) (Table 1). Some representative ^{1}H-NMR spectra are collected in the supplementary information (Fig. S1).

2.3. Kinase inhibition activity evaluation

All the synthetized indolinone compounds were evaluated as

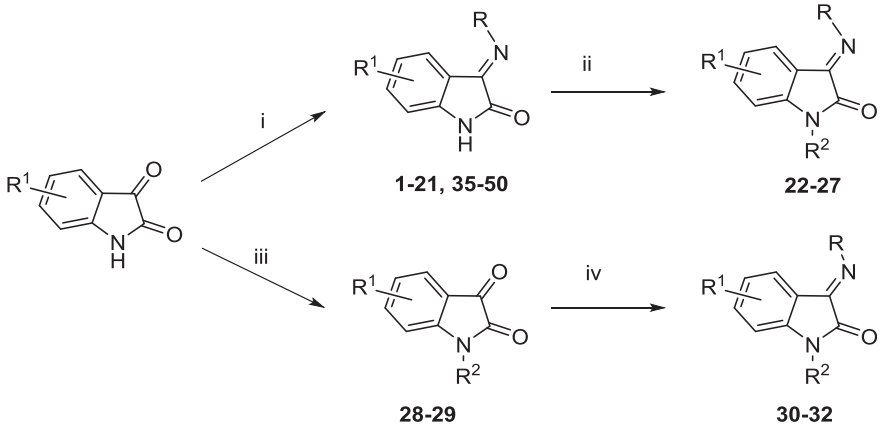

Scheme 1. Reaction conditions: i) MMT-K10, MW, 10–100 °C, 5–30 min; ii) EtOH, KOH, SO_4Me_2 or BrBn; iii) DMF, NaH, CH_3I or BrBn; iv) MW, 110 °C, 0.5–1.5 h.

Table 1
Reaction yields, *E:Z* isomeric ratios, predicted blood-brain barrier (BBB) penetration and biological activity (LRRK2 inhibition and Wnt signal enhancement) of synthetized isatines **1**–**50**.

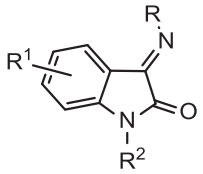

Comp. No.	R	R^1	R^2	Yield	*E:Z* ratio	LRRK2 %inh@10 μM	LRRK2 IC_{50} (μM)[a]	LRRK2 G2019S %inh @10 μM	LRRK2 G2019S IC_{50} (μM)[a]	BBB
1	3-NO_2-Ph-	H	H	50%	63:37	19%	-	–	–	–
2	4-OMe-Ph-	H	H	75%	83:17	63%	2.17	75%	2.33	CNS+
3	4-Br-Ph-	H	H	84%	77:23	11%	-	–	–	–
4	Ph-	H	H	86%	83:17	71%	3.65	70%	2.98	CNS+
5	2-OMe-Ph-	H	H	27%	83:17	15%	-	–	–	–
6	2-CF_3-Ph-	H	H	53%	62:38	12%	-	–	–	–
7	2-Cl-Ph-	H	H	4%	77:23	30%	-	–	–	–
8	2-F-Ph-	H	H	60%	67:33	60%	2.34	73%	3.29	CNS+
9	3-Cl-Ph-	H	H	10%	63:37	39%	-	–	–	–
10	4-F-Ph-	H	H	71%	67:33	71%	3.18	69%	3.69	CNS+
11	4-CN-Ph-	H	H	56%	64:36	45%	15.40	–	–	–
12	4-NO_2-Ph-	H	H	24%	64:36	66%	7.27	–	–	–
13	4-$N(Me)_2$-Ph-	H	H	84%	76:24	76%	3.79	64%	3.11	CNS+
14	2,4-$(OMe)_2$-Ph-	H	H	47%	83:17	15%	-	–	–	–
15	3,4-$(OMe)_2$-Ph-	H	H	65%	83:17	3%	-	–	–	–
16	-$N(Ph)_2$	H	H	74%	95:5	96%	0.11	93%	0.29	CNS+
17	-$CH(Ph)_2$	H	H	48%	35:65	−1%	-	–	–	–
18	-NHPh	H	H	24%	14:86	23%	-	–	–	–
19	-Piperidine	H	H	86%	46:54	79%	1.34	77%	2.21	CNS+
20	-Morpholine	H	H	59%	88:12	74%	1.70	61%	6.68	CNS+
21	-N(Bn)(Ph)	H	H	93%	44:56	71%	3.83	73%	3.67	CNS+
22	-$N(Ph)_2$	H	Me	86%	91:9	49%	5.76	40%	–	–
23	-$N(Ph)_2$	H	Bn	29%	80:20	40%	6.98	40%	–	–
24	-Piperidine	H	Me	24%	49:51	−3%	-	–	–	–
25	-Piperidine	H	Bn	47%	33:67	1%	-	–	–	–
26	-Morpholine	H	Me	32%	59:41	6%	-	–	–	–
27	-Morpholine	H	Bn	93%	45:55	2%	-	–	–	–
28	–	H	Bn	82%	–	−1%	-	–	–	–
29	–	H	Me	52%	–	−15%	-	–	–	–
30	4-F-Ph-	H	Bn	87%	77:23	1%	-	–	–	–
31	4-OMe-Ph-	H	Bn	72%	80:20	13%	-	–	–	–
32	4-Br-Ph-	H	Me	49%	76:24	9%	-	–	–	–
33	-$N(Ph)_2$	5-Cl	H	59%	85:15	96%	0.01	96%	0.05	n.d.
34	-$N(Ph)_2$	5-F	H	40%	96:4	97%	0.02	99%	0.12	n.d.
35	-$N(Ph)_2$	7-Cl	H	72%	92:8	17%	-	–	–	–
36	-$N(Ph)_2$	5-Br	H	49%	91:9	91%	0.02	93%	0.03	n.d.
37	-$N(Ph)_2$	5-OCF_3	H	8%	100:0	61%	5.35	40%	21.5	–
38	-$N(Ph)_2$	5-OMe	H	6%	100:0	100%	0.13	95%	0.31	CNS+
39	-Piperidine	5-Cl	H	91%	92:8	91%	0.28	91%	0.57	CNS+
40	-Piperidine	5-F	H	83%	30:70	77%	1.50	79%	2.01	CNS+
41	-Piperidine	7-Cl	H	47%	25:75	11%	-	–	–	–
42	-Piperidine	5-Br	H	6%	21:79	92%	0.49	93%	0.54	CNS+
43	-Piperidine	5-OMe	H	51%	41:59	94%	0.76	85%	1.11	CNS+
44	-Morpholine	5-Cl	H	77%	26:74	78%	1.20	83%	1.46	CNS+
45	-Morpholine	5-F	H	12%	30:70	66%	3.65	61%	5.40	CNS+
46	-Morpholine	7-Cl	H	56%	26:74	7%	-	–	–	–
47	-Morpholine	5-Br	H	10%	17:83	91%	1.33	88%	1.02	CNS+
48	-Morpholine	5-OCF_3	H	83%	12:88	54%	8.74	40%	7.49	–
49	-Morpholine	5-OMe	H	32%	38:62	72%	6.02	64%	5.93	–
50	-Morpholine	5-I	H	57%	30:70	95%	0.55	95%	0.51	CNS+

[a] Standard compound Lrrk2-in-1: IC_{50} values: 0.02 μM and 0.02 μM in LRRK2 and LRRK2 G2019S respectively.

potential inhibitors of LRRK2. The assays were performed using LifeTechnologies Adapta® methodology according to the procedure described in the experimental section. This is a fluorescent-based immunoassay for the detection of ADP formed by the kinase reaction. Human recombinant LRRK2 and its substrate known as LRRKtide peptide (sequence: RLGRDKYKTLRQIRQ) were incubated in the presence or absence of inhibitors, and the ADP formed was quantified using specific antibodies resulting in a TR-FRET signal variation. All the compounds were assayed twice at a fixed concentration of 10 μM using the commercial compound lrrk2-in-1 as reference standard. When the percentage of inhibition was more than 50%, the dose response curve was determined and the IC_{50} value calculated. Moreover, compounds that inhibit LRRK2 were also assayed in human recombinant LRRK2 G2019S, the most common LRRK2 mutation in familial PD patients [20], following the same protocol. This mutation results in an increase of kinase activity that is linked to the severity degree of the pathology [21]. Some of the compounds here synthesized showed a marked inhibition on LRRK2 and LRRK2 G2019S with IC_{50} values in the nano/submicro molar range, similar to the reference compound lrrk2-in-

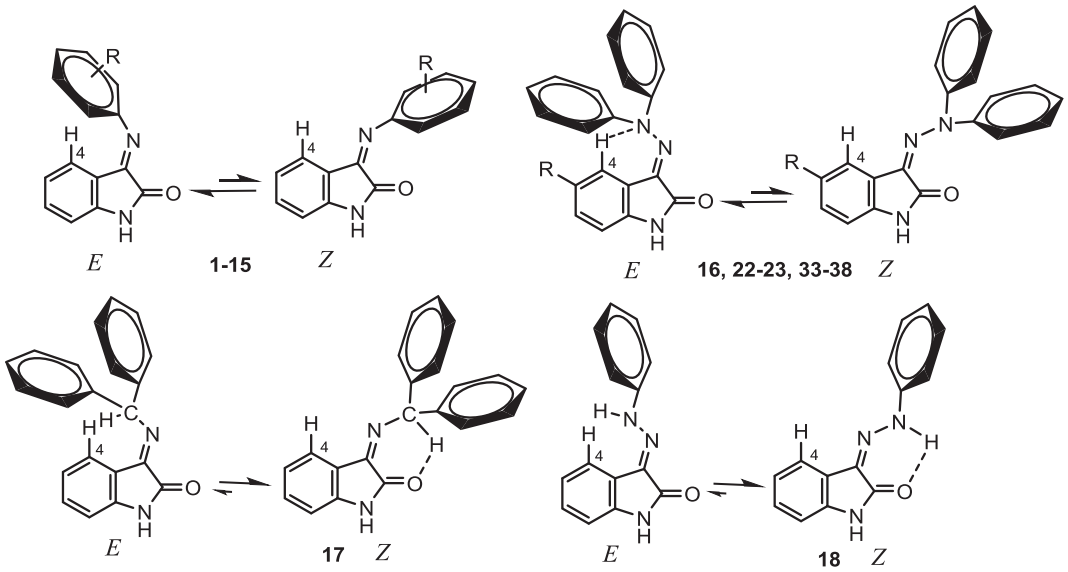

Fig. 3. Different *E:Z* isomers of the indolinone imino and hydrazone derivatives.

1. Generally, if a compound was able to inhibit LRRK2, it was also able to inhibit this mutated form with similar potency even with PD-linked mutation being located in activation loop [22]. All the data are collected in Table 1.

Since one of the main challenges in kinase inhibitor discovery is the selectivity, and being aware that the central scaffold of our compounds is also present in other protein kinase inhibitors (Fig. 1), we performed a kinase profiling with the first indolinone-like LRRK2 inhibitor here prepared (**16**) with an IC_{50} value in the sub-micromolar range (IC_{50} = 0.11 μM) to be sure that we are working with selective LRRK2 inhibitors. We selected a panel of fifty different human protein kinases and tested the compound at a fixed concentration of 10 μM. In this panel, those kinases previously inhibited by different compounds containing the indolinone framework, as those depicted in Fig. 1, were included. Thus the inhibitory activity on different CK1 isoforms and EGFR, IGF1R and PDGFR alpha as representatives of tyrosin kinases were evaluated. Detailed experimental background such as ATP concentration and quantity of each enzyme used are described in the supporting information (Table S2). Selected protein kinases and the percentage of kinase activity remained after compound **16** treatment is depicted in Fig. 4. High selectivity towards LRRK2 inhibition was observed for indolinone derivative **16**, which only showed a slight inhibition on the FMS-like tyrosine kinase 3 (FLT-3), pointing to a selective family of inhibitors. FLT-3 is involved and aberrantly active in acute myeloid leukemia [23]. To assure this selectivity profile, a second indolinone was selected to run the same panel. In that case, our criteria were to be a potent inhibitor and to have good drug like properties such the permeability in the central nervous system (CNS). Kinase selectivity for this family of compounds was confirmed when the isatin-like compound **38** was used (Fig. 4).

2.4. Structure-activity relationships and molecular modeling studies

These first results revealed clear structure-activity relationships providing important clues for further optimization. Among the 3-phenylimino-indolinone derivatives, substitution position in the

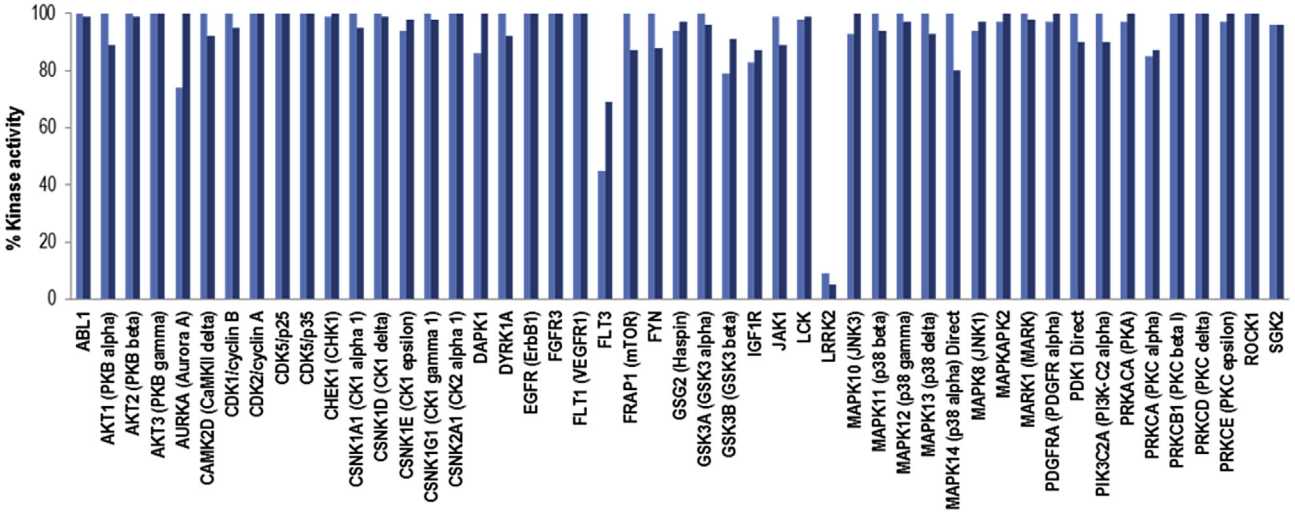

Fig. 4. Kinase profiling of indolinone **16** (light blue) and **38** (dark blue) at compound fixed concentration of 10 μM. (For interpretation of the references to colour in this figure legend, the reader is referred to the web version of this article.)

phenyl ring was critical for activity. Only para-substituents were tolerated. Inhibition of LRRK2 was found for derivatives **2** and **10**–**13**, all of them with different chemical moieties in position 4 of the phenyl ring. By contrast, there was a lack of potency when these substituents are in orto- and/or meta-position (compounds **1, 5**–**9, 14**–**15**). An exception was observed in indolinone **8** with a fluorine atom attached in orto-position to the phenyl ring. This compound had an IC_{50} value of 2.34 μM, which is in the same range to that of derivative **4** (IC_{50} = 3.65 μM) in which the phenyl ring is not substituted. That may be explained by the similarity of the size of fluorine atom to that of the hydrogen one.

More effective for kinase inhibition was the introduction of a hydrazone spacer instead the imino linker. In those cases an increase in the inhibition of LRRK2 was observed (compounds **16, 19**–**21** *versus* **1**–**15**). This effect was clearly revealed by the submicromolar activity of indolinone **16** and the complete lack of activity of compound **17**. The only difference between these two compounds was the replacement of a carbon atom by a nitrogen one, resulting in the shifting from imino to hydrazone moiety.

Regarding the indolinone ring, greater variations in the biological activity were found when different modifications in this heterocyclic core are introduced. For example, the NH group was completely necessary for LRRK2 inhibition and when it was modified by alkylation, kinase inhibition was lost or decreased by more than one order of magnitude (compounds **23**–**27** and **31** *versus* indolinones **16, 19, 20** and **2**). Substitution in position 7 of the heterocyclic core completely abolished activity of compounds **35, 41** and **46**, presumably causing the loss of interaction with LRRK2. However, an increase in the inhibition potency was found when position 5 of indolinone framework was modified by different chemical groups such as halides or different ethers (compounds **33, 34, 36**–**40, 42**–**45, 47**–**50**). In some cases, such as compounds **33, 34** and **36,** we obtained very potent LRRK2 inhibitors with IC_{50} values in the low two digit nanomolar range.

In order to gain insight into the binding mode of this new family of potent LRRK2 inhibitors, and looking for clues to assist in the lead-to-candidate optimization, a docking study using Glide XP (Schrödinger suite program) that allows examining a potential binding mode to the enzyme was carried out. The kinase domain of LRRK2 has not been crystallized but a LRRK2 homology model has recently been published [24]. We reproduced the LRRK2 homology model using the crystal structure of Janus Kinase 2 as template and the human LRRK2 sequence retrieved from Swiss-Prot (see supplementary material) following the published protocol.

All the compounds showed a similar binding mode in the catalytic site of LRRK2. In Fig. 5A the docking of indolinone **33** is shown, as a representative example. The most important interaction was governed by the dual hydrogen bond between Lys 1906 and two features of the indolinone ring: the carbonyl group in position 2 and the nitrogen atom of the hydrazine attached to the heterocycle. This molecular orientation allowed both the formation of a halogen bond between the Asp1887 and the halide atom in position 5 of the indolinone, and the possibility of a hydrogen bond between the Asp 2017 and the heterocyclic NH. This binding mode with the same molecule orientation and key interactions was also present in compounds with piperidine (**39**) or morpholine in the hydrazone linker (Fig. 5B). This binding mode might explain the better value of activity of those compounds with chemical groups in position 5.

Considering the protein surface and druggable cavities, in the catalytic site exits two pockets where additional van der Waals interactions with the ligand may increase enzymatic potency. The first one at the back of Lys 1906 and Glu 1920 was fully occupied with one of the phenyl rings of diphenyl amino compounds that may be responsible for the higher potency of these derivatives in comparison with their piperidine and morpholine analogs. However, the six-membered ring present in these last compounds was oriented totally towards the second cavity, pointing to a new direction where current molecules may be modified to potentially increase hydrophobic interactions (Fig. 6).

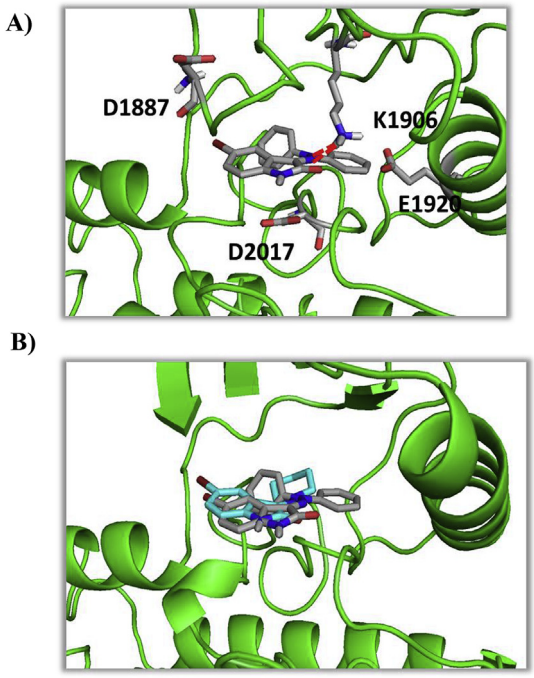

Fig. 5. A) Binding mode of indolinone **33** into catalytic site of LRRK2. B) Superposition of compounds **33** (blue color) and **39** bound to LRRK2. (For interpretation of the references to colour in this figure legend, the reader is referred to the web version of this article.)

2.5. Prediction of blood brain barrier (BBB) permeability

As one of the main obstacles for the treatment of the diseases of the central nervous system (CNS) is the drug's penetration into the blood-brain barrier (BBB) at therapeutic concentrations, we decided to explore the prediction of our top indolinone-based LRRK2 inhibitors to penetrate into the human BBB. Parallel artificial membrane permeability assay (PAMPA) is a high-throughput technique developed to predict passive permeability through biological membranes [25], and we used this methodology to evaluate the BBB permeability of our LRRK2 inhibitors. The first step consists of an assay validation comparing the human reported permeabilities (*Pe*) values of several marketed drugs with the experimental data obtained by using this methodology (Fig. S2 supporting information). A good correlation between experimental-described values was obtained *Pe* (exp) = 1.1324 *Pe* (bibl.) = 1.0056 (R^2 = 0.9689). From this equation and following the pattern established in the literature for BBB permeation prediction [26], we could classify compounds as CNS + when they present a permeability $>3.54 \times 10^{-6}$ cm s^{-1}. The *in vitro* permeabilities (*Pe*) of commercial drugs through lipid membrane extract together with those belonging to indolinones derivatives were determined as described in Table 1 and Supporting information Table S3. Although calculated prediction to cross the BBB was positive for all the compounds, solubility problems were encountered for compounds **33, 34** and **36** and the prediction of BBB permeability was not possible to be determined. The low solubility of these compounds may be explained considering the predicted values of octanol/

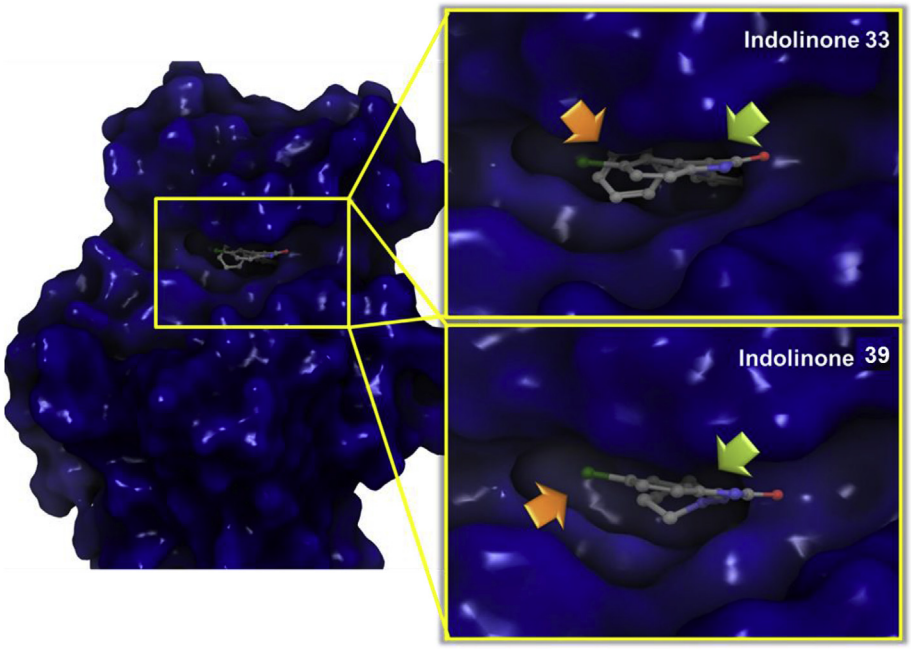

Fig. 6. Indolinones **33** and **39** bound to LRRK2. Green and orange arrows show the two back cavities present in the active site of LRRK2. (For interpretation of the references to colour in this figure legend, the reader is referred to the web version of this article.)

water partition coefficient (log p), polar surface area (PSA) and aqueous solubility (log S) calculated by QuickPro program for compounds **33, 34, 36** and **38** (see supporting information Table S4). More than one order of magnitude was found in log S between **38** and **33, 34** and **36** although their chemical structures are very similar, pointing to a better solubility for derivative **38.** Thus, as many of the LRRK2 inhibitors tested are predicted to cross the BBB by PAMPA assay they have potential for further pharmaceutical development including *in vivo* studies of CNS diseases.

2.6. Neurogenic properties of LRRK2 inhibitors

Adult NSCs continuously generate neurons throughout life in two brain regions: the subgranular zone of the hippocampus and the V-SVZ, adjacent to the lateral ventricles. The V-SVZ is the largest germinal region in the adult mammalian brain and generates olfactory bulb interneurons and oligodendrocytes and in the case of the human brain, it could also be the source of neuroblasts and interneurons found in the adjacent striatum [27]. Thus, the finding of new molecules able to increase the neurogenic potential of the VZ-SVZ niche, especially in the case of PD patients with alterations in LRRK2 activity, is of great relevance.

To determine if some of the LRKK2 inhibitors described in Table 1 could have an impact on neurogenesis we selected five indolinone-like LRRK2 inhibitors taking in consideration enzymatic activity, solubility properties, compound availability and chemical diversity. In total, piperidine, morpholine and diphenylamino substituents of the hydrazine moiety were present in compounds **19, 20, 38, 44** and **45**, selected for these studies.

As NSCs and neural progenitors cultured *in vitro* have the ability to grow as spheres [28], we used primary NSCs and neural progenitors isolated from the subventricular zone of adult mice and cultured them in the presence or absence of the above mentioned compounds at a fixed concentration of 5 μM. We investigated whether addition of indolinone-like LRRK2 inhibitors impacted the formation of neurospheres after the dissociated NSCs and neural progenitors were growing for 3 days in the presence of mitogens (FGF and EGF). As shown in Fig. 7, the size of neurospheres (estimated as total area of the neurospheres) was significantly higher in those cultures treated with the selected small molecules (indolinones **19, 20, 38, 44** and **45**), compared to controls treated with DMSO (Fig. 7C; control normalized: 100 ± 16.7%; LRRK inhibitors from 118.5 ± 5% (compound **38**) to 141.5 ± 9% (indolinone **45**). This increase of up to 1.4-fold in the total area of the formed neurospheres could be related to an increase in the size of individual neurospheres due to an increase in proliferation or to an increase in the number of neurospheres caused by an increase in the number of cells with the ability to form neurospheres. The number of neurospheres formed in the presence of the tested LRRK2 inhibitors was similar to those formed in control conditions (Fig. 7D). Thus, the inhibition of LRRK2, using specific indolinone-derivatives, promotes the proliferation of NSCs and neural progenitors from adult SVZ grown as neurospheres.

3. Conclusions

LRRK2, an enigmatic enzyme implicated in both familial and idiopathic PD risk, may be also play an important role in adult neurogenesis through the Wnt signaling pathway.

Since the discovery of the adult neurogenesis great research efforts have been made to decipher its role and implications in health and pathological conditions. Currently, it is recognized that aging, neurodegenerative and some mental diseases are associated with a decrease in brain neurogenesis, although the exact relevance of this decrease to disease etiology and pathogenesis remains debated. Thus, small molecules able to modulate neurogenesis and neuroplasticity, are intensively being pursued as valuable pharmacological probes and as new potential therapeutic agents for these unmet conditions or diseases [29].

With the aim of translating these discoveries into therapeutics, we have designed new indoline-derived LRRK2 inhibitors with predicted brain permeability and determine their potential as regulators of adult neurogenesis in neural stem cells isolated from the ventricular-subventricular zone. Therefore, these inhibitors of

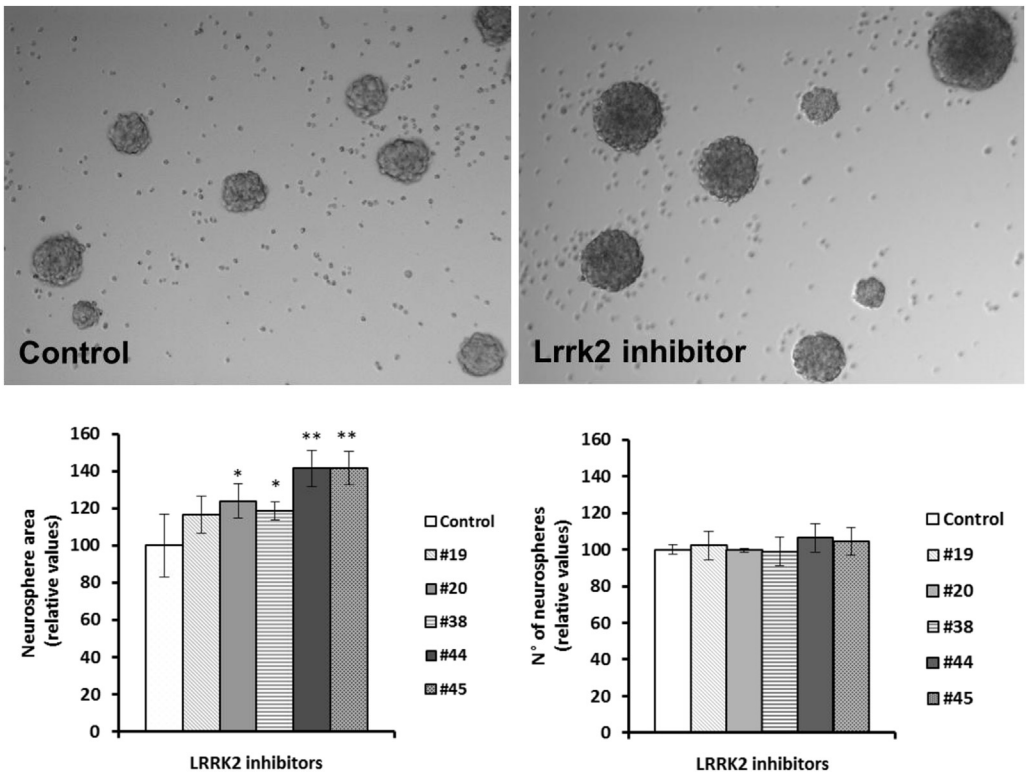

Fig. 7. Effects of LRRK2 inhibitors on neurosphere formation. (A–B) Representative bright field micrographs showing the size of primary neurospheres after 3 days in culture in the presence of DMSO as a control (A) or LRRK2 inhibitor **38** (B). (C–D) Quantitative analysis of the neurospheres in culture. The total neurosphere area was measured (C) and the number of neurospheres was counted (D) in each field using an especially designed macro for IMAGE J. Results are mean value ± SEM, represented as relatives to control value (=100), of five different fields each one from triplicates and from three independent experiments. Bar in A: 100 μm $^{*}p \leq 0.05$; $^{**}p \leq 0.005$.

the activity of LRRK2 may be considered as pharmacological probes to study the potential neuroregeneration of the damaged brain. Further studies are in progress to show the regenerative potential of LRRK2 inhibitors in *in vivo* models.

4. Experimental section

4.1. Chemistry

Reagents were purchased from commercial sources and used without further purification. Melting points were determined with a Mettler Toledo MP70 apparatus. Crude residues were purified with the indicated solvent as eluent by flash column chromatography carried out at medium pressure using silica gel (E. Merck, Grade 60, particle size 0.040–0.063 mm, 230–240 mesh ASTM) or IsoleraOne flash purification system from Biotage. Compounds were detected with UV light (254 nm). ^{1}H-NMR spectra were obtained on the Bruker AVANCE-300 spectrometer working at 300 MHz or on a Varian INOVA 400 spectrometer working at 400 MHz. Typical spectral parameters: spectral width 16 ppm, pulse width 9 μs (57°), data size 32 K. ^{13}C-NMR experiments were carried out on the Bruker AVANCE-300 spectrometer operating at 75 MHz or on a Varian INOVA 400 spectrometer working at 100 MHz. The acquisition parameters: spectral width 16 kHz, acquisition time 0.99 s, pulse width 9 μs (57°), data size 32 K. Chemical shifts are reported in values (ppm) relative to internal Me_4Si and *J* values are reported in Hz. HPLC analyses were performed on Alliance Waters 2690 equipment, with a UV detector photodiode array Waters 2996 with MS detector MicromassZQ (Waters), using an Sunfire column C18, 3.5 μm (50 mm × 4.6 mm) and acetonitrile and MilliQ water (with 0.1% formic acid) as mobile phase. The standard gradient consisted of a 5 min run from 15% to 95% of acetonitrile at a flow rate of 1 mL/min. Elemental analyses were performed by the analytical department at CENQUIOR (CSIC), and the results obtained were within ±0.4% of the theoretical values. The microwave assisted syntheses were carried out using a Biotage Initiator eight single-mode cavity instrument from Biotage. Experiments were performed with temperature control mode in sealed microwave process vials. The temperature was measured with an IR sensor on the outside of the reaction vessel. Stirring was provided by an *in situ* magnetic stirrer.

General procedure for compounds 1–21, 30–50: Following the procedure described by Pandey et al. [17] with some modifications. A mixture of the isatin derivative (1 eq), the corresponding amine derivative (1 eq) and MMT-K10 (20 mg for 1 mmol of the isatin derivative) and toluene if necessary, was heated under microwave irradiation (6–90 min, 100–110 °C). After cooling to room temperature, ethyl acetate (50 mL) was added and the mixture was extracted with a saturated solution of $NaHCO_3$ (50 mL x 3). Finally, the organic phase was dried over magnesium sulfate and the solvent evaporated under reduced pressure. The residue was chromatographed as indicated in each case.

In case the amine was in hydrochloride form, the amine derivative (1 eq) was stirred with triethylamine (1 eq) and toluene (3 mL) for 1 h at room temperature.

(*E,Z*)-3-((3-Nitrophenyl)imino)indolin-2-one (1): Reagents: isatin (250 mg, 1.7 mmol), 3-nitroaniline (234.7 mg, 1.7 mmol), MMT-K10 (34 mg) and toluene (1 mL). Reaction conditions: 15 min at 100 °C. The crude product was purified by IsoleraOne (water/acetonitrile 7:3) to afford an orange solid (226.1 mg, 50%), ratio *E*/*Z*: 63:37, mp: 217–218 °C. Isomer *E*: ^{1}H-NMR (400 MHz, DMSO-d_6): δ 10.98 (s, 1 H), 8.10 (ddd, $J = 8.1, 2.2, 0.9$ Hz, 1H), 7.85 (t,

J = 2.1 Hz, 1H), 7.75 (t, J = 8.0 Hz, 1H), 7.51–7.41 (m, 1H), 7.36 (td, J = 7.8, 1.2 Hz, 1H), 6.90 (d, J = 7.1 Hz, 1H), 6.72 (td, J = 7.7, 1.0 Hz, 1H), 6.34 (d, J = 7.4 Hz, 1H). ^{13}C-NMR (100 MHz, DMSO-d_6): δ 163.9, 157.1, 152.1, 149.4, 148.2, 135.7, 131.9, 126.4, 125.2, 122.6, 120.2, 116.3, 113.0, 112.4. Isomer *Z*: ^{1}H-NMR (400 MHz, DMSO-d_6): δ 10.98 (s, 1H), 7.95 (ddd, J = 8.2, 2.4, 1.0 Hz, 1H), 7.85 (t, J = 2.1 Hz, 1H), 7.61 (d, J = 7.5 Hz, 2H), 7.59 (t, J = 8.1 Hz, 1H), 7.51–7.41 (m, 1H), 7.07 (td, J = 7.5, 0.6 Hz, 1H), 6.87 (d, J = 6.8 Hz, 1H). ^{13}C-NMR (100 MHz, DMSO-d_6): δ 159.2, 155.5, 151.3, 148.6, 147.2, 135.5, 130.5, 126.4, 124.0, 123.1, 121.6, 119.3, 114.2, 111.7. MS (ESI+): *m/z* 268 [M+H]. Anal. $C_{14}H_9N_3O_3$ (C, H, N, O).

(*E,Z*)-3-((4-Methoxyphenyl)imino)indolin-2-one (2): Reagents: isatin (600 mg, 4.1 mmol), 4-methoxyaniline (502.3 mg, 4.1 mmol), MMT-K10 (81.6 mg) and toluene (1 mL). Reaction conditions: 30 min at 100 °C. The crude product was purified by column cromatography (chloroform/methanol 10:1) to afford an orange-yellow solid (769.2 mg, 75%), ratio *E*/*Z*: 83:17, mp: 237–238 °C (lit [30] 238 °C).

(*E,Z*)-3-((4-Bromophenyl)imino)indolin-2-one (3): Reagents: isatin (250 mg, 1.7 mmol), 4-bromoaniline (292.3 mg, 1.7 mmol), MMT-K10 (34 mg) and toluene (1 mL). Reaction conditions: 10 min at 100 °C. The final product was obtained without further purification as an orange solid (433.5 mg, 85%), ratio *E*/*Z*: 77:23, mp: 241–242 °C (lit [17] 242 °C).

(*E,Z*)-3-(Phenylimino)indolin-2-one (4): Reagents: isatin (250 mg, 1.7 mmol), aniline (158.2 mg, 1.7 mmol), MMT-K10 (34 mg) and toluene (1 mL). Reaction conditions: 10 min at 100 °C. The crude product was purified by IsoleraOne (water/acetonitrile 7:3) to afford a yellow solid (323.7 mg, 86%), ratio *E*/*Z*: 83:17, mp: 231–232 °C (lit [31] 232–234 °C).

(*E,Z*)-3-((2-Methoxyphenyl)imino)indolin-2-one (5): Reagents: isatin (250 mg, 1.7 mmol), 2-methoxyaniline (209.2 mg, 1.7 mmol), MMT-K10 (34 mg) and toluene (1 mL). Reaction conditions: 10 min at 100 °C. The crude product was purified by IsoleraOne (water/acetonitrile 7:3) to afford an orange solid (116.3 mg, 27%), ratio *E*/*Z*: 83:17, mp: 179–180 °C (lit [32] 177–179 °C).

(*E,Z*)-3-((2-(Trifluoromethyl)phenyl)imino)indolin-2-one (6): Reagents: isatin (250 mg, 1.7 mmol), 2-trifluoromethylaniline (273.7 mg, 1.7 mmol), MMT-K10 (34 mg) and toluene (1 mL). Reaction conditions: 20 min at 100 °C. The crude product was purified by IsoleraOne (water/acetonitrile 7:3) to afford an orange solid (262.3 mg, 53%), ratio *E*/*Z*: 62:38, mp: 144–145 °C (lit [33] 144 °C).

(*E,Z*)-3-((2-Chlorophenyl)imino)indolin-2-one (7): Reagents: isatin (250 mg, 1.7 mmol), 2-chloroaniline hydrochloride (278.6 mg, 1.7 mmol), MMT-K10 (34 mg) and toluene (1 mL). Reaction conditions: 12 min at 100 °C. The crude product was purified by IsoleraOne (water/acetonitrile 7:3) to afford a yellow solid (16.6 mg, 4%), ratio *E*/*Z*: 77:23, mp: 236–237 °C (lit [34] 238 °C).

(*E,Z*)-3-((2-Fluorophenyl)imino)indolin-2-one (8): Reagents: isatin (250 mg, 1.7 mmol), 2-fluoroaniline (188.8 mg, 1.7 mmol) and MMT-K10 (34 mg). Reaction conditions: 6 min at 100 °C. The crude product was purified by IsoleraOne (water/acetonitrile 7:3) to afford an orange solid (246.5 mg, 60%), ratio *E*/*Z*: 67:33, mp: 198–199 °C (lit [35] 198–199 °C).

(*E,Z*)-3-((3-Chlorophenyl)imino)indolin-2-one (9): Reagents: isatin (250 mg, 1.7 mmol), 3-chloroaniline hydrochloride (278.6 mg, 1.7 mmol), MMT-K10 (34 mg) and toluene (1 mL). Reaction conditions: 6 min at 100 °C. The crude product was purified by IsoleraOne (water/acetonitrile 7:3) to afford an orange solid (45.1 mg, 10%), ratio *E*/*Z*: 63:37, mp: 219–220 °C (lit [35] 221–223 °C).

(*E,Z*)-3-((4-Fluorophenyl)imino)indolin-2-one (10): Reagents: isatin (250 mg, 1.7 mmol), 4-fluoroaniline (188.8 mg, 1.7 mmol), MMT-K10 (34 mg) and toluene (1 mL). Reaction conditions: 6 min at 100 °C. The crude product was purified by IsoleraOne (water/acetonitrile 7:3) to afford a yellow solid (289.5 mg, 71%), ratio *E*/*Z*: 67:33, mp: 216–217 °C (lit [36] 210–216 °C).

(*E,Z*)-4-((2-oxoindolin-3-ylidene)amino)benzonitrile (11): Reagents: isatin (250 mg, 1.7 mmol), 4-aminobenzonitrile (200.7 mg, 1.7 mmol), MMT-K10 (34 mg) and toluene (1 mL). Reaction conditions: 30 min at 100 °C. The crude product was purified by IsoleraOne (water/acetonitrile 1:1) to afford an orange solid (236.9 mg, 56%), ratio *E*/*Z*: 64:36, mp: 257–258 °C (lit [37] 257–259 °C).

(*E,Z*)-3-((4-Nitrophenyl)imino)indolin-2-one (12): Reagents: isatin (250 mg, 1.7 mmol), 4-nitroaniline (234.7 mg, 1.7 mmol), MMT-K10 (34 mg) and toluene (1 mL). Reaction conditions: 30 min at 100 °C. The crude product was purified by IsoleraOne (water/acetonitrile 7:3) to afford an orange solid (110.5 mg, 24%), ratio *E*/*Z*: 64:36, mp: 236–237 °C (lit [35] 231–236 °C).

(*E,Z*)-3-((4-(Dimethylamino)phenyl)imino)indolin-2-one (13): Reagents: isatin (250 mg, 1.7 mmol), *N*′,*N*′-dimethylbenzene-1,4-diamine (231.4 mg, 1.7 mmol), MMT-K10 (34 mg) and toluene (1 mL). Reaction conditions: 30 min at 100 °C. The crude product was purified by IsoleraOne (water/acetonitrile 7:3) to afford an orange solid (380.1 mg, 84%), ratio *E*/*Z*: 76:24, mp: 224 °C (lit [38] 220 °C, decom.).

(*E,Z*)-3-((2,4-Dimethoxyphenyl)imino)indolin-2-one (14) [39]: Reagents: isatin (250 mg, 1.7 mmol), 2,4-dimethoxyaniline (260.3 mg, 1.7 mmol), MMT-K10 (34 mg) and toluene (1 mL). Reaction conditions: 6 min at 100 °C. The crude product was purified by IsoleraOne (water/acetonitrile 3:2) to afford an orange-red solid (223.2 mg, 47%), ratio *E*/*Z*: 83:17, mp: 216–217 °C.

(*E,Z*)-3-((3,4-Dimethoxyphenyl)imino)indolin-2-one (15): Reagents: isatin (250 mg, 1.7 mmol), 3,4-dimethoxyaniline (260.3 mg, 1.7 mmol), MMT-K10 (34 mg) and toluene (1 mL). Reaction conditions: 6 min at 100 °C. The crude product was purified by IsoleraOne (water/acetonitrile 4:1) to afford an orange-red solid (312.7 mg, 65%), ratio *E*/*Z*: 83:17, mp: 265–266 °C. Isomer *E*: ^{1}H-NMR (400 MHz, DMSO-d_6): δ 10.91 (s, 1H), 7.31 (td, J = 7.7, 1.4 Hz, 1H), 7.03–6.99 (m, 1H), 6.86 (dt, J = 7.9, 0.8 Hz, 1H), 6.74 (d, J = 1.9 Hz, 1H), 6.70–6.64 (m, 2H), 6.51 (dd, J = 8.4, 2.3 Hz, 1H), 3.76 (s, 3H), 3.68 (s, 3H). ^{13}C-NMR (100 MHz, DMSO-d_6): δ 164.4, 155.2, 150.2, 147.4, 147.1, 144.1, 134.9, 125.8, 122.4, 116.4, 113.1, 112.1, 109.9, 103.8, 56.4, 56.1. Isomer *Z*: ^{1}H-NMR (400 MHz, DMSO-d_6): δ 10.80 (s, 1H), 7.54–7.49 (m, 1H), 7.38 (td, J = 7.7, 1.3 Hz, 1H), 7.03–6.99 (m, 1H), 6.93–6.88 (m, 1H), 6.86 (dt, J = 7.9, 0.8 Hz, 1H), 6.81 (dt, J = 7.7, 0.8 Hz, 1H), 6.74 (d, J = 1.9 Hz, 1H), 3.74 (s, 3H), 3.69 (s, 3H). MS (ESI+): *m/z* 283 [M+H]. Anal. $C_{16}H_{14}N_2O_3$ (C, H, N, O).

(*E,Z*)-3-(2,2-Diphenylhydrazono)indolin-2-one (16): Reagents: isatin (250 mg, 1.7 mmol), 2,2-diphenylhydrazine hydrochloride (220.7 mg, 1.7 mmol), MMT-K10 (34 mg), triethylamine (171.9 mg, 1.7 mmol) and toluene (3 mL). Reaction conditions: 6 min at 100 °C. The crude product was purified by IsoleraOne (water/acetonitrile 7:3) to afford a green-yellow solid (394.8 mg, 74%), ratio *E*/*Z*: 95:5, mp: 246–248 °C (lit [40] 245–246 °C).

(*E,Z*)-3-(Benzhydrylimino)indolin-2-one (17) [41]: Reagents: isatin (250 mg, 1.7 mmol), diphenylmethanamine (311.3 mg, 1.7 mmol) and MMT-K10 (34 mg). Reaction conditions: 20 min at 100 °C. The crude product was purified by IsoleraOne (water/acetonitrile 7:3) to afford an orange-yellow solid (255.1 mg, 48%), ratio *E*/*Z*: 35:65, mp: 173–174 °C.

(*E,Z*)-3-(2-(4-Tolyl)hydrazono)indolin-2-one (18): Reagents: isatin (250 mg, 1.7 mmol), 4-tolylhydrazine hydrochloride (269.5 mg, 1.7 mmol), triethylamine (171.9 mg, 1.7 mmol), MMT-K10 (34 mg) and toluene (3 mL). Reaction conditions: 10 min at 100 °C. The crude product was purified by IsoleraOne (water/acetonitrile 7:3) to afford an orange solid (104.1 mg, 24%), ratio *E*/*Z*: 14:86, mp: 224–225 °C. Isomer *Z*: ^{1}H-NMR (400 MHz, DMSO-d_6): δ 12.71 (s, 1H), 10.97 (s, 1H), 7.50 (d, J = 7.3 Hz, 1H), 7.33 (d, J = 8.5 Hz, 2H), 7.23 (td, J = 7.7, 1.3 Hz, 1H), 7.18 (d, J = 8.5 Hz, 2H),

7.04 (tdd, J = 7.6, 1.6, 0.9 Hz, 1H), 6.95–6.88 (m, 1H), 2.24 (s, 3H). ^{13}C-NMR (100 MHz, DMSO-d_6): δ 163.9, 140.9, 140.2, 132.7, 130.6, 128.9, 127.6, 122.5, 121.9, 119.1, 114.7, 111.1, 21.1. MS (ESI+): m/z 252 [M + 1]. Anal. $C_{15}H_{13}N_3O$ (C, H, N, O).

(*E,Z*)-3-(Piperidin-1-ylimino)indolin-2-one (19): Reagents: isatin (250 mg, 1.7 mmol), piperidin-1-amine (170.2 mg, 1.7 mmol) and MMT-K10 (34 mg). Reaction conditions: 10 min at 100 °C. The crude product was purified by IsoleraOne (water/acetonitrile 4:1) to afford an orange solid (335.0 mg, 86%), ratio *E*/*Z*: 46:54, mp: 142–143 °C (lit [40] 141–142 °C).

(*E,Z*)-3-(Morpholinoimino)indolin-2-one (20): Reagents: isatin (250 mg, 1.7 mmol), morpholin-4-amine (173.6 mg, 1.7 mmol) and MMT-K10 (34 mg). Reaction conditions: 10 min at 100 °C. The crude product was purified by IsoleraOne (water/acetonitrile 4:1) to afford an orange solid (354.5 mg, 59%), ratio *E*/*Z*: 88:12, mp: 184–186 °C (lit [40] 186–188 °C).

(*E,Z*)-3-(2-Benzyl-2-phenylhydrazono)indolin-2-one (21): Reagents: isatin (350 mg, 2.4 mmol), 1-benzyl-1-phenylhydrazine hydrochloride (558.4 mg, 2.37 mmol), MMT-K10 (47.6 mg), triethylamine (239.8 mg, 2.37 mmol) and toluene (3 mL). Reaction conditions: 40 min at 110 °C. The crude product was purified by column chromatography (dichloromethane/methanol 30:1) to afford an orange solid (29.2 mg, 4%), ratio *E*/*Z*: 56:44, mp: 157–158 °C. Isomer *E*/*Z*: ^{1}H-NMR (400 MHz, DMSO-d_6): δ 10.75 (s, 1H), 10.66 (s, 1H), 7.61–7.47 (m, 4H), 7.40–7.32 (m, 1H), 7.33–6.96 (m, 18H), 6.91 (dd, J = 7.9, 0.8 Hz, 1H), 6.83–6.77 (m, 2H), 6.61 (td, J = 7.8, 1.1 Hz, 1H), 6.27 (s, 2H), 6.26–6.20 (m, 1H), 5.23 (s, 2H). ^{13}C-NMR (100 MHz, DMSO-d_6): δ 166.1, 159.2, 147.5, 147.2, 143.8, 140.2, 139.0, 138.3, 137.5, 131.2, 129.8, 129.1, 128.8, 128.2, 128.0, 127.5, 127.1, 126.2, 125.7, 125.4, 124.7, 124.3, 123.4, 122.2, 121.6, 120.8, 120.0, 118.1, 116.4, 112.9, 110.7, 110.2, 63.6, 58.5. MS (ESI+): m/z 328 [M+H]. Anal. $C_{21}H_{17}N_3O$ (C, H, N, O).

(*E/Z*)-1-Benzyl-3-((4-fluorophenyl)imino)indolin-2-one (30) [42]: Reagents: 1-benzylindoline-2,3-dione (200 mg, 0.8 mmol), 4-fluoroaniline (93.7 mg, 0.8 mmol), MMT-K10 (27 mg) and toluene (1 mL). Reaction conditions: 30 min at 100 °C. The crude product was purified by IsoleraOne (water/acetonitrile 10:1) to afford an orange solid (243.6 mg, 88%), ratio *E*/*Z*: 77:23, mp: 200–201 °C.

(*E*/*Z*)-3-((4-Methoxyphenyl)imino)-1-phenylindolin-2-one (31) [43]: Reagents: 1-benzylindoline-2,3-dione (100 mg, 0.4 mmol), 4-methoxyaniline (527 mg, 0.4 mmol), MMT-K10 (13 mg) and toluene (5 mL). Reaction conditions: 1 h at 100 °C. The crude product was purified by column chromatography (dichloromethane) to afford an orange solid (103 mg, 72%), ratio *E*/*Z*: 80:20, mp: 153–154 °C.

(*E*/*Z*)-3-((4-Bromophenyl)imino)-1-methylindolin-2-one (32): Reagents: 1-methylindoline-2,3-dione (205 mg, 1.3 mmol), 4-bromoaniline (218 mg, 1.3 mmol), MMT-K10 (26 mg) and toluene (5 mL). Reaction conditions: 90 min at 100 °C. The crude product was purified by column chromatography (chloroform) to afford an orange solid (196 mg, 49%), ratio *E*/*Z*: 76:24, mp: 148–149 °C (lit [44] 148 °C).

(*E,Z*)-5-Chloro-3-(2,2-diphenylhydrazono)indolin-2-one (33): Reagents: 5-chloroisatin (250 mg, 1.4 mmol), 2,2-diphenylhydrazine hydrochloride (254.0 mg, 1.4 mmol), triethylamine (139.0 mg, 1.4 mmol), MMT-K10 (27 mg) and toluene (6 mL). Reaction conditions: 30 min at 100 °C. The crude product was purified by IsoleraOne (water/acetonitrile 7:3) to afford a yellow solid (284.1 mg, 59%), ratio *E*/*Z*: 85:15, mp: 305–306 °C (lit [40] 305–306 °C).

(*E,Z*)-5-Fluoro-3-(2,2-diphenylhydrazono)indolin-2-one (34): Reagents: 5-fluoroisatin (250 mg, 1.5 mmol), 2,2-diphenylhydrazine hydrochloride (279.0 mg, 1.5 mmol), triethylamine (153.0 mg, 1.5 mmol), MMT-K10 (30 mg) and toluene (5 mL). Reaction conditions: 1 h at 100 °C. The crude product was purified by column chromatography (dichloromethane) to afford a brown solid (138 mg, 27%), ratio *E*/*Z*: 96:4, mp: 228–229 °C. Isomer *E*: ^{1}H-NMR (400 MHz, DMSO-d_6): δ 10.65 (s, 1H), 7.49 (m, 4H), 7.34 (m, 6H), 6.94 (ddd, J = 9.1, 8.5, 2.6 Hz, 1H), 6.73 (dd, J = 8.5, 4.7 Hz, 1H), 4.86 (dd, J = 10.5, 2.6 Hz, 1H). ^{13}C-NMR (100 MHz, DMSO-d_6): δ 166.6, 157.37 (d, J = 234.0 Hz), 146.0, 139.9 (d, J = 1.5 Hz), 131.3, 130.3, 127.2, 123.9, 117.1 (d, J = 8.8 Hz), 116.8 (d, J = 23.7 Hz), 112.7 (d, J = 27.8 Hz), 111.1 (d, J = 8.1 Hz). MS (ESI+): m/z 332 [M + 1]. Anal. $C_{20}H_{14}FN_3O$ (C, H, N, O).

(*E,Z*)-7-Chloro-3-(2,2-diphenylhydrazono)indolin-2-one (35): Reagents: 7-chloroisatin (250 mg, 1.4 mmol), 2,2-diphenylhydrazine hydrochloride (254.0 mg, 1.4 mmol), triethylamine (139.0 mg, 1.4 mmol), MMT-K10 (27 mg) and toluene (2 mL). Reaction conditions: 1 h at 100 °C. The crude product was purified by IsoleraOne (water/acetonitrile 4:1) to afford a yellow solid (344 mg, 72%), ratio *E*/*Z*: 92:8, mp: 208–209 °C. Isomer *E*: ^{1}H-NMR (400 MHz, DMSO-d_6): δ 11.05 (s, 1H), 7.46 (m, 4H), 7.32 (m, 6H), 7.15 (dd, J = 8.2, 0.9 Hz, 1H), 6.41 (t, J = 8.0 Hz, 1H), 5.23 (dd, J = 7.9, 0.9 Hz, 1H). ^{13}C-NMR (100 MHz, DMSO-d_6): δ 166.5, 145.9, 141.0, 131.9, 130.3, 129.8, 127.1, 124.0, 123.8, 122.8, 122.2, 118.3. MS (ESI+): m/z 350 [M + 3H], 348 [M+H]. Anal. $C_{20}H_{14}ClN_3O$ (C, H, N, O).

(*E/Z*)-5-Bromo-3-(2,2-diphenylhydrazono)indolin-2-one (36): Reagents: 5-bromoisatin (500 mg, 2.2 mmol), 2,2-diphenylhydrazine hydrochloride (485.5 mg, 2.2 mmol), MMT-K10 (44 mg), triethylamine (222.6 mg, 2.2 mmol) and toluene (3 mL). Reaction conditions: 10 min at 110 °C. The crude product was purified by IsoleraOne (water/acetonitrile 7:3) to afford a yellow solid (419.4 mg, 49%), ratio *E*/*Z*: 91:9, mp: 242–244 °C. Isomer *E*: ^{1}H-NMR (500 MHz, DMSO-d_6): δ 10.75 (s, 1H), 7.48–7.42 (m, 4H), 7.36–7.31 (m, 6H), 7.23 (dd, J = 8.2, 2.1 Hz, 1H), 6.69 (d, J = 8.2 Hz, 1H), 5.09 (d, J = 2.1 Hz, 1H). ^{13}C-NMR (125 MHz, DMSO-d_6): δ 165.9, 145.5, 142.3, 132.4, 130.1, 129.9, 127.8, 127.1, 123.7, 117.9, 113.0, 112.0. Isomer *Z*: ^{1}H-NMR (500 MHz, DMSO-d_6): δ 10.75 (s, 1H), 7.63–7.62 (m, 1H), 7.48 (m, 4H), 7.36–7.31 (m, 6H), 7.18 (m, 1H), 6.73 (d, J = 8.7 Hz, 1H). MS (ESI+): m/z 394 [M + 3H], 392 [M+H]. Anal. $C_{20}H_{14}BrN_3O$ (C, H, N, O).

(*E*)-3-(2,2-Diphenylhydrazono)-5-(trifluoromethoxy)indolin-2-one (37): Reagents: 5-trifluoromethoxyisatin (500 mg, 2.2 mmol), 2,2-diphenylhydrazine hydrochloride (485.5 mg, 2.2 mmol), MMT-K10 (44 mg), triethylamine (222.6 mg, 2.2 mmol) and toluene (3 mL). Reaction conditions: 40 min at 110 °C. The crude product was purified by column chromatography (dichloromethane/methanol 40:1) to afford a yellow solid (48 mg, 8%), mp: 230–231 °C. ^{1}H-NMR (300 MHz, DMSO-d_6):δ 10.82 (s, 1H), 7.48–7.33 (m, 10H), 7.13–7.09 (m, 1H), 6.83 (d, J = 8.6 Hz, 1 H), 4.99 (d, J = 1.6 Hz, 1H). ^{13}C-NMR (100 MHz, DMSO-d_6):δ 165.8, 145.2, 141.9, 129.9, 129.6, 123.2, 123.0, 118.6, 116.4, 110.5. MS (ESI+): m/z 398 [M+H]. Anal. $C_{21}H_{14}F_3N_3O_2$ (C, H, N, O).

(*E*)-3-(2,2-Diphenylhydrazono)-5-methoxyindolin-2-one (38): Reagents: 5-methoxyisatin (500 mg, 2.8 mmol), 2,2-diphenylhydrazine hydrochloride (622.4 mg, 2.8 mmol), MMT-K10 (56.4 mg), triethylamine (284.5 mg, 2.8 mmol) and toluene (3 mL). Reaction conditions: 40 min at 110 °C. The crude product was purified by column chromatography (dichloromethane/methanol 40:1) to afford a yellow solid (20 mg, 6%), mp: 203–204 °C. ^{1}H-NMR (400 MHz, DMSO-d_6): δ 10.45 (s, 1H), 7.46–7.41 (m, 4H), 7.30–7.24 (m, 6H), 6.70 (dd, J = 8.5, 2.4 Hz, 1H), 6.60 (d, J = 8.5 Hz, 1H), 5.27 (d, J = 2.4 Hz, 1H), 3.30 (s, 3H). ^{13}C-NMR (100 MHz, DMSO-d_6): δ 166.4, 154.4, 146.5, 137.7, 135.4, 130.3, 130.2, 123.6, 56.2.MS (ESI+): m/z 344 [M+H]. Anal. $C_{21}H_{17}N_3O_2$ (C, H, N, O).

(*E,Z*)-5-Chloro-3-(piperidin-1-ylimino)indolin-2-one (39): Reagents: 5-chloroisatin (250 mg, 1.4 mmol), piperidin-1-amine (137.0 mg, 1.4 mmol), MMT-K10 (27 mg) and toluene (5 mL). Reaction conditions: 30 min at 100 °C. The final product was obtained without further purification as a yellow solid (327 mg, 91%), ratio *E*/

Z: 18:82, mp: 193–194 °C. Isomer *Z*: ^{1}H-NMR (400 MHz, DMSO-d_6): δ 10.63 (s, 1H), 7.18 (d, *J* = 2.2 Hz, 1H), 7.04 (dd, *J* = 8.2, 2.2 Hz, 1H), 6.73 (d, *J* = 8.2 Hz, 1H), 4.08–3.95 (m, 4H), 1.73–1.54 (m, 6H). ^{13}C-NMR (100 MHz, DMSO-d_6): δ 159.1, 137.5, 130.4, 126.0, 125.8, 121.4, 117.6, 111.0, 58.6, 26.7, 23.8. Isomer *E*: ^{1}H-NMR (400 MHz, DMSO-d_6): δ 10.72 (s, 1H), 7.31 (dd, *J* = 8.3, 2.1 Hz, 1H), 7.16 (d, *J* = 2.1 Hz, 1H), 6.86 (d, *J* = 8.3 Hz, 1H), 3.30–3.25 (m, 4H), 1.73–1.54 (m, 6H). ^{13}C-NMR (100 MHz, DMSO-d_6): δ 165.7, 142.2, 137.3, 128.2, 126.1, 124.9, 117.5, 112.4, 56.8, 25.7, 23.8. MS (ESI+): *m*/*z* 266 [M + 3H], 264 [M+H]. Anal. $C_{13}H_{14}ClN_3O$ (C, H, N, O).

(*E*,*Z*)-5-Fluoro-3-(piperidin-1-ylimino)indolin-2-one (40): Reagents: 5-fluoroisatin (250 mg, 1.5 mmol), piperidin-1-amine (152.0 mg, 1.5 mmol), MMT-K10 (30 mg) and toluene (5 mL). Reaction conditions: 30 min at 100 °C. The crude product was purified by column chromatography (dichloromethane/methanol 150:1) to afford a yellow solid (311.6 mg, 83%), ratio *E*/*Z*: 30:70, mp: 169–170 °C. Isomer *Z*: ^{1}H-NMR (400 MHz, DMSO-d_6): δ 10.55 (s, 1H), 7.01 (ddd, *J* = 8.9, 6.7, 2.7 Hz, 1.5H), 6.87 (m, 1.5H), 6.73 (dd, *J* = 8.4, 4.4 Hz, 1H), 4.04 (m, 4H), 1.77–1.48 (m, 9H). ^{13}C-NMR (100 MHz, DMSO-d_6): δ 159.4, 158.6 (d, *J* = 234.4 Hz), 135.0 (d, *J* = 1.3 Hz), 127.8 (d, *J* = 8.8 Hz), 122.4, 112.8 (d, *J* = 24.0 Hz), 110.3 (d, *J* = 8.2 Hz), 105.0 (d, *J* = 25.4 Hz), 58.5, 26.6, 23.8. Isomer *E*: ^{1}H-NMR (400 MHz, DMSO-d_6): δ 10.64 (s, 0.5H), 7.15 (ddd, *J* = 9.4, 8.5, 2.6 Hz, 0.5H), 7.01 (ddd, *J* = 8.9, 6.7, 2.7 Hz, 1.5H), 6.87 (m, 1.5H), 3.30 (m, 2H), 1.77–1.48 (m, 9H). ^{13}C-NMR (100 MHz, DMSO-d_6): δ 166.0, 158.2 (d, *J* = 235.8 Hz), 139.9, 138.2, 117.2 (d, *J* = 23.5 Hz), 116.8 (d, *J* = 8.3 Hz), 112.4 (d, *J* = 26.1 Hz), 111.7, 56.8, 25.7, 23.9. MS (ESI+): *m*/*z* 248 [M+H]. Anal. $C_{13}H_{14}FN_3O$ (C, H, N, O).

(*E*,*Z*)-7-Chloro-3-(piperidin-1-ylimino)indolin-2-one (41): Reagents: 7-chloroisatin (250 mg, 1.4 mmol), piperidin-1-amine (137 mg, 1.4 mmol), MMT-K10 (27 mg) and toluene (5 mL). Reaction conditions: 30 min at 100 °C. The crude product was purified by column chromatography (dichloromethane/methanol 100:1) to afford a yellow solid (171.6 mg, 47%), ratio *E*/*Z*: 25:75, mp: 151–152 °C. Isomer *Z*: ^{1}H-NMR (400 MHz, DMSO-d_6): δ 10.93 (s, 1H), 7.19 (ddd, *J* = 7.6, 4.5, 1.0 Hz, 1H), 7.09 (dd, *J* = 8.1, 1.0 Hz, 1H), 6.88 (ddd, *J* = 8.1, 7.5, 0.5 Hz, 1H), 4.82–3.77 (m, 4H), 1.75–1.53 (m, 6H). ^{13}C-NMR (100 MHz, DMSO-d_6): δ 159.0, 135.9, 130.5, 128.1, 126.2, 122.6, 116.7, 114.0, 58.6, 26.7, 23.7. Isomer *E*: ^{1}H-NMR (400 MHz, DMSO-d_6): δ 11.02 (s, 1H), 7.33 (dd, *J* = 8.2, 0.9 Hz, 1H), 7.19 (ddd, *J* = 7.6, 4.5, 1.0 Hz, 1H), 7.09–7.00 (m, 1H), 3.31–3.25 (m, 1H), 1.75–1.53 (m, 9H). ^{13}C-NMR (100 MHz, DMSO-d_6): δ 165.9, 140.8, 137.3, 124.1, 123.5, 122.1, 118.1, 115.2, 56.8, 25.7, 23.9. MS (ESI+): *m*/*z* 266 [M + 3H], 264 [M+H]. Anal $C_{13}H_{14}ClN_3O$ (C, H, N, O).

(*E*,*Z*)-5-Bromo-3-(piperidin-1-yimino)indolin-2-one (42): Reagents: 5-Bromoisatin (500 mg, 2.2 mmol), piperidin-1-amine (220.4 mg, 2.2 mmol), MMT-K10 (44 mg), triethylamine (222.6 mg, 2.2 mmol) and toluene (3 mL). Reaction conditions: 40 min at 110 °C. The crude product was purified by column chromatography (dichloromethane/methanol 30:1) to afford a yellow solid (42.2 mg, 6%), ratio *E*/*Z*: 23:77, mp: 168–170 °C. Isomer *Z*: ^{1}H-NMR (400 MHz, DMSO-d_6): δ 10.63 (s, 1H), 7.30 (d, *J* = 2.1 Hz, 1H), 7.16 (dd, *J* = 8.2, 2.0 Hz, 1H), 6.68 (d, *J* = 8.2, 0.5 Hz, 1 H), 4.08 (t, *J* = 5.6 Hz, 4H), 1.72–1.55 (m, 6H). ^{13}C-NMR (100 MHz, DMSO-d_6): δ 158.9, 142.6, 137.6, 128,8, 120.4, 113.5, 111.5, 58.6, 26.7, 23.8. Isomer *E*: ^{1}H-NMR (400 MHz, DMSO-d_6): δ 10.73 (s, 1H), 7.45 (dd, *J* = 8.3, 2.1 Hz, 1H), 7.30 (d, *J* = 2.1 Hz, 1H), 6.82 (d, *J* = 8.2 Hz, 1H), 3.29 (t, *J* = 5.7 Hz, 1H), 1.72–1.55 (m, 9H).^{13}C-NMR (100 MHz, DMSO-d_6): δ 165.5, 121.2, 56.8, 25.7. MS (ESI+): *m*/*z* 310 [M + 3H], 308 [M+H]. Anal. $C_{13}H_{14}BrN_3O$ (C, H, N, O).

(*E*,*Z*)-5-Methoxy-3-(piperidin-1-ylimino)indolin-2-one (43): Reagents: 5-Methoxyisatin (350.0 mg, 2.0 mmol), piperidin-1-amine (198.3, 2.0 mmol) y MMT-K10 (39.6 mg) and toluene (3 mL). Reaction conditions: 40 min at 110 °C. The final product was obtained without further purification as an orange solid (260 mg, 51%), ratio *E*/*Z*: 40:60, mp: 173–175 °C. Isomer *Z*: ^{1}H-NMR (400 MHz, DMSO-d_6): δ 10.33 (s, 1H), 6.93–6.84 (m, 1H), 6.80 (dd, *J* = 1.6, 0.9 Hz, 1H), 6.65–6.60 (m, 1H), 3.91–3.89 (m, 4H), 3.67 (s, 3H), 1.83–1.38 (m, 6H).^{13}C-NMR (100 MHz, DMSO-d_6): δ 159.4, 155.2, 141.6, 133.0, 117.1, 112.3, 111.5, 103.9, 58.4, 56.0, 26.6, 24.1. Isomer *E*: ^{1}H-NMR (400 MHz, DMSO-d_6): δ 10.43 (s, 1H), 6.93–6.84 (m, 1H), 6.78 (dd, *J* = 8.2, 0.7 Hz, 1 H), 6.65–6.60 (m, 1H), 3.71 (s, 3H), 3.20–3.15 (m, 4H), 1.83–1.38 (m, 6H). ^{13}C-NMR (100 MHz, DMSO-d_6): δ 165.9, 155.1, 126.9, 110.40, 56.4, 56.2, 23.9, 23.8. MS (ESI+): *m*/*z* 260 [M + 1]. Anal. $C_{14}H_{17}N_3O_2$ (C, H, N, O).

(*E*,*Z*)-5-Chloro-3-(morpholinoimino)indolin-2-one (44): Reagents: 5-chloroisatin (250 mg, 1.4 mmol), morpholin-4-amine (141 mg, 1.4 mmol), MMT-K10 (27 mg) and toluene (5 mL). Reaction conditions: 1 h at 100 °C. The crude product was purified by column chromatography (dichloromethane/methanol 100:1) to afford a yellow solid (280.8 mg, 77%), ratio *E*/*Z*: 26:74, mp: 192–193 °C. Isomer *Z*: ^{1}H-NMR (400 MHz, DMSO-d_6): δ 10.79 (s, 1H), 7.25 (d, *J* = 2.1 Hz, 1H), 7.14 (dd, *J* = 8.2, 2.2 Hz, 1H), 6.79 (d, *J* = 8.2 Hz, 1H), 4.04 (dd, *J* = 6.2, 3.6 Hz, 4H), 3.80 (m, 4H). ^{13}C-NMR (100 MHz, DMSO-d_6): δ 159.1, 138.1, 127.3, 127.0, 126.0, 124.5, 118.3, 111.3, 66.6, 57.7. Isomer *E*: ^{1}H-NMR (400 MHz, DMSO-d_6): δ 10.84 (s, 1H), 7.39 (dd, *J* = 8.4, 2.1 Hz, 1H), 7.29 (d, *J* = 2.1 Hz, 1H), 6.90 (d, *J* = 8.3 Hz, 1H), 3.80 (m, 4H), 3.29 (m, 4H). ^{13}C-NMR (100 MHz, DMSO-d_6): δ 165.3, 143.0, 141.1, 131.5, 126.3, 125.8, 117.1, 112.6, 66.1, 56.0. MS (ESI+): *m*/*z* 268 [M + 3H], 266 [M+H]. Anal. $C_{12}H_{12}ClN_3O$ (C, H, N, O).

(*E*,*Z*)-5-Fluoro-3-(morpholinoimino)indolin-2-one (45): Reagents: 5-fluoroisatin (250 mg, 1.5 mmol), morpholin-4-amine (155 mg, 1.5 mmol), MMT-K10 (30 mg) and toluene (5 mL). Reaction conditions: 30 min at 100 °C. The crude product was purified by column chromatography (dichloromethane/methanol 100:1) to afford a yellow solid (149.2 mg, 40%), ratio *E*/*Z*: 30:70, mp: 191–192 °C. Isomer *Z*: ^{1}H-NMR (400 MHz, DMSO-d_6): δ 10.66 (s, 1H), 7.01 (dd, *J* = 8.7, 2.7 Hz, 1H), 6.90 (ddd, *J* = 9.8, 8.4, 2.7 Hz, 1H), 6.76–6.70 (m, 1H), 4.03–3.96 (m, 4H), 3.77–3.71 (m, 4H). ^{13}C-NMR (100 MHz, DMSO-d_6): δ 159.4, 158.7 (d, *J* = 235.1 Hz), 135.8 (d, *J* = 1.1 Hz), 126.9 (d, *J* = 9.0 Hz), 125.7 (d, *J* = 3.3 Hz), 113.9 (d, *J* = 24.0 Hz), 110.7 (d, *J* = 8.4 Hz), 105.7 (d, *J* = 25.2 Hz), 66.6, 57.6. Isomer *E*: ^{1}H-NMR (400 MHz, DMSO-d_6): δ 10.70 (s, 1H), 7.17 (ddd, *J* = 9.5, 8.5, 2.6 Hz, 1H), 7.10 (dd, *J* = 8.8, 2.6 Hz, 1H), 6.85 (dd, *J* = 8.6, 4.5 Hz, 1H), 3.82–3.77 (m, 4H), 3.27–3.21 (m, 4H). ^{13}C-NMR (100 MHz, DMSO-d_6): δ 165.6, 158.2 (d, *J* = 236.8 Hz), 141.9 (d, *J* = 2.5 Hz), 140.6 (d, *J* = 1.6 Hz), 118.4 (d, *J* = 23.6 Hz), 116.3 (d, *J* = 8.6 Hz), 113.5 (d, *J* = 25.8 Hz), 112.0 (d, *J* = 8.1 Hz), 66.1, 56.0. MS (ESI+): *m*/*z* 250 [M+H]. Anal. $C_{12}H_{12}FN_3O_2$ (C, H, N, O).

(*E*,*Z*)-7-Chloro-3-(morpholinoimino)indolin-2-one (46): Reagents: 7-chloroisatin (250 mg, 1.4 mmol), morpholin-4-amine (141 mg, 1.4 mmol), MMT-K10 (27 mg) and toluene (5 mL). Reaction conditions: 1 h at 100 °C. The crude product was purified by column chromatography (dichloromethane/methanol 100:1) to afford a yellow solid (204.6 mg, 56%), ratio *E*/*Z*: 26:74, mp: 178–179 °C (lit [40] 180–181 °C).

(*E*,*Z*)-5-Bromo-3-(morpholinoimino)indolin-2-one (47): Reagents: 5-bromoisatin (500 mg, 2.2 mmol), morpholin-4-amine (224.7 mg, 2.2 mmol), MMT-K10 (44 mg) and toluene (3 mL). Reaction conditions: 40 min at 110 °C. The crude product was purified by column chromatography (dichloromethane/methanol 30:1) to afford a yellow solid (28 mg, 10%), ratio *E*/*Z*: 25:75, mp: 191–193 °C. Isomer *Z*: ^{1}H-NMR (400 MHz, DMSO-d_6): δ 10.78 (s, 1H), 7.35 (d, *J* = 2.0 Hz, 1H), 7.24 (dd, *J* = 8.2, 2.0 Hz, 1H), 6.73 (d, *J* = 8.2 Hz, 1H), 4.02 (t, *J* = 4.9 Hz, 4H), 3.85–3.71 (m, 4H). ^{13}C-NMR (100 MHz, DMSO-d_6): δ 158.9, 141.1, 138.4, 129.8, 124.3, 121.0, 113.7, 111.9, 66.7, 57.7. Isomer *E*: ^{1}H-NMR (400 MHz, DMSO-d_6): δ 10.82 (s, 1H), 7.49 (dd, *J* = 8.3, 1.9 Hz, 1H), 7.39 (d, *J* = 2.0 Hz, 1H), 6.84 (d, *J* = 8.2 Hz,

1H), 3.85–3.71 (m, 4H), 3.20 (m, 4H). ^{13}C-NMR (100 MHz, DMSO-d_6): δ 165.2, 143.4, 134.4, 127.8, 114.0, 66.1, 56.0. MS (ESI+): *m/z* 313 [M + 3H], 310 [M+H]. Anal. $C_{12}H_{12}BrN_3O_2$ (C, H, N, O).

(*E,Z*)-5-(Trifluoromethoxy)-3-morpholinoimino)indolin-2-one (48): Reagents: 5-trifluoromethoxyisatin (350.0 mg, 1.5 mmol), morpholin-4-amine (268.4, 1.5 mmol), MMT-K10 (30.2 mg) and toluene (3 mL). Reaction conditions: 40 min at 110 °C. The final product was obtained without further purification as a yellow solid (392.1 mg, 83%), ratio *E*/*Z*: 12:88, mp: 153–154 °C. Isomer *E*/*Z*: ^{1}H-NMR (400 MHz, DMSO-d_6): δ 10.81 (s, 1H), 7.13 (dd, *J* = 2.5, 1.2 Hz, 1H), 7.10–7.02 (m, 1H), 6.80 (d, *J* = 8.4 Hz, 1H), 4.05–3.95 (m, 4H), 3.78–3.73 (m, 4H). ^{13}C-NMR (100 MHz, DMSO-d_6): δ 159.3, 143.7, 138.2, 126.9, 124.5, 121.0 (q, *J* = 254 Hz), 120.4, 112.6, 110.7, 66.6, 57.3. MS (ESI+): *m/z* 316 [M+H]. Anal. $C_{13}H_{12}F_3N_3O_3$ (C, H, N, O).

(*E,Z*)-5-Methoxy-3-(morpholinoimino)indolin-2-one (49): Reagents: 5-methoxyisatin (350.0 mg, 2.0 mmol), morpholin-4-amine (202.2 mg, 2.0 mmol), MMT-K10 (39.6 mg) and toluene (3 mL). Reaction conditions: 40 min at 110 °C. The final product was obtained without further purification as an orange solid (167 mg, 32%), ratio *E*/*Z*: 30:70, mp: 168–170 °C. Isomer *Z*: ^{1}H-NMR (500 MHz, DMSO-d_6): δ 10.49 (s, 1H), 6.95–6.94 (m, 1H), 6.71 (dd, *J* = 8.4, 2.4 Hz, 1H), 6.68 (dd, *J* = 8.4, 0.7 Hz, 1H), 3.96–3.85 (m, 4H), 3.79–3.73 (m, 4H), 3.69 (s, 3H). ^{13}C-NMR (125 MHz, DMSO-d_6): δ 159.3, 155.3, 144.1138.3, 126.0, 112.7, 110.3, 104.5, 66.5, 57.3, 56.1. Isomer *E*: ^{1}H-NMR (500 MHz, DMSO-d_6): δ 10.52 (s, 1H), 6.93 (d, *J* = 2.6 Hz, 1H), 6.85 (d, *J* = 2.2 Hz, 1H), 6.80 (dd, *J* = 7.9, 0.9 Hz, 1H), 3.84–3.78 (m, 4H), 3.70 (s, 3H), 3.21–3.15 (m, 4H). ^{13}C-NMR (125 MHz, DMSO-d_6): δ 165.1, 155.2, 133.9, 128.3, 118.1, 117.9, 111.7, 66.1, 56.2, 55.8. MS (ESI+): *m/z* 262 [M+H]. Anal. $C_{13}H_{15}N_3O_3$ (C, H, N, O).

(*E,Z*)-5-Iodo-3-(morpholinoimino)indolin-2-one (50): Reagents: 5-Iodoisatin (350.0 mg, 1.3 mmol), morpholin-4-amine (226.7 mg, 1.3 mmol), MMT-K10 (25.6 mg) and toluene (3 mL). Reaction conditions: 40 min at 110 °C. The final product was obtained without further purification as a yellow solid (246 mg, 72%), ratio *E*/*Z*: 30:70, mp: 198–199 °C. Isomer *Z*: ^{1}H-NMR (300 MHz, DMSO-d_6): δ 10.76 (s, 1H), 7.65–7.63 (dd, *J* = 8.2, 1.7 Hz, 1H), 7.42–7.40 (dd, *J* = 8.1, 1.8 Hz, 1H), 6.63 (d, *J* = 8.1 Hz, 1H), 4.01–3.99 (m, 4H), 3.77–3.75 (m, 4H). ^{13}C-NMR (100 MHz, DMSO-d_6): δ 158.4, 141.2, 138.3, 134.9, 127.8, 126.1, 111.7, 84.0, 66.4, 57.5. Isomer *E*: ^{1}H-NMR (300 MHz, DMSO-d_6): δ 10.76 (s, 1H), 7.65–7.63 (dd, *J* = 8.2, 1.7 Hz, 1H), 7.57 (d, *J* = 1.7 Hz, 1H), 6.74 (d, *J* = 8.2 Hz, 1H), 3.77–3.75 (m, 4H), 3.25–3.23 (m, 4H). ^{13}C-NMR (100 MHz, DMSO-d_6): δ 164.7, 143.6, 138.3, 133.9, 113.3, 85.02, 65.8, 55.8 MS (ESI+): *m/z* 358 [M+H]. Anal. $C_{12}H_{12}IN_3O_2$ (C, H, N, O).

Synthesis of N-substituted compounds 22–28: For the synthesis of these compounds we followed the procedure described by Ottoni et al. [19] In our case, the crude was purified by column chromatography using chloroform as eluent.

(*E,Z*)-3-(2,2-Diphenylhydrazono)-1-methylindolin-2-one (22): Reagents: (*E,Z*)-3-(2,2-diphenylhydrazono)indolin-2-one (100 mg, 0.3 mmol), dimethyl sulfate (50.2 mg, 0.4 mmol), KOH (22.3 mg, 0.4 mmol), ethanol (3 mL) and acetone (3 mL). Final product: orange solid (273.9 mg, 86%), ratio *E*/*Z*: 91:9, m.p: 193–194 °C. (lit. [45] 194–195 °C).

(*E,Z*)-1-Benzyl-3-(2,2-Diphenylhydrazono)indolin-2-one (23): Reagents: (*E,Z*)-3-(2,2-diphenylhydrazono)indolin-2-one (100 mg, 0.3 mmol), benzyl bromide (68.2 mg, 0.4 mmol), KOH (22.3 mg, 0.4 mmol), ethanol (3 mL) and acetone (3 mL). Final product: orange solid (110.5 mg, 96%), ratio *E*/*Z*: 80:20, m.p: 177–178 °C. Isomer *E*: ^{1}H-NMR (400 MHz, DMSO-d_6): δ 7.52–7.40 (m, 4H), 7.35–7.26 (m, 9H), 7.26–7.16 (m, 2H), 7.06 (td, *J* = 7.8, 1.2 Hz, 1H), 6.91–6.81 (m, 1H), 6.42 (td, *J* = 7.7, 1.1 Hz, 1H), 5.34 (ddd, *J* = 7.9, 1.2, 0.5 Hz, 1H), 4.94 (s, 2H). ^{13}C-NMR (100 MHz, DMSO-d_6): δ 165.4, 146.6, 146.2, 143.7, 137.1, 132.3, 130.7, 129.8, 129.2, 128.0, 127.8, 126.9, 125.6, 122.8, 121.9, 109.8, 43.3. MS (ESI+): *m/z* 404 [M+H]. Anal. $C_{27}H_{21}N_3O_2$ (C, H, N, O).

(*E,Z*)-1-Methyl-3-(piperidin-1-ylimino)indolin-2-one (24): Reagents: (*E,Z*)-3-(piperidin-1-ylimino)indolin-2-one (250 mg, 1.1 mmol), dimethyl sulfate (137 mg, 1.1 mmol), KOH (76 mg, 1.4 mmol), ethanol (10 mL) and acetone (10 mL). Final product: orange oil (78 mg, 29%), ratio *E*/*Z*: 49:61. Isomer *Z*: ^{1}H-NMR (400 MHz, DMSO-d_6): δ 7.31 (ddd, *J* = 7.5, 1.2, 0.6 Hz, 1H), 7.17 (td, *J* = 7.7, 1.2 Hz, 1H), 6.96 (m, 2H), 4.00 (t, 4H), 3.18 (s, 3H), 1,72 (m, 4H), 1,61 (m, 2H). ^{13}C-NMR (100 MHz, DMSO-d_6): δ 157.4, 140.3, 139.7, 127.1, 124.9, 122.1, 118.1, 108.6, 58.3, 26.6, 25.6, 23.9. Isomer *E*: ^{1}H-NMR (400 MHz, DMSO-d_6): δ 7.39 (td, *J* = 7.7, 1.2 Hz, 1H), 7.35 (ddd, *J* = 7.7, 1.3, 0.6 Hz, 1H), 7.13 (td, *J* = 7.6, 1.0 Hz, 1H), 7.07 (m, 1H), 3.25 (m, 4H), 3.17 (s, 3H), 1.72 (m, 4H), 1,61 (m, 2H). ^{13}C-NMR (100 MHz, DMSO-d_6): δ 164.5, 145.0, 139.7, 131.5, 125.7, 123.0, 122.9, 109.7, 56.7, 26.6, 26.5, 23.9. MS (ESI+): *m/z* 244 [M+H]. Anal. $C_{14}H_{17}N_3O_2$ (C, H, N, O).

(*E,Z*)-1-Benzyl-3-(piperidin-1-ylimino)indolin-2-one (25): Reagents: (*E,Z*)-3-(piperidin-1-ylimino)indolin-2-one (250 mg, 1.1 mmol), benzyl bromide (186 mg, 1.1 mmol), KOH (78 mg, 1.4 mmol), ethanol (10 mL) and acetone (10 mL). Final product: yellow solid (85 mg, 24%), ratio *E*/*Z*: 33:67, m.p: 127–128 °C. Isomer *Z*: ^{1}H-NMR (400 MHz, DMSO-d_6): δ 7.31 (m, 6H), 7.09 (td, *J* = 7.8, 1.2 Hz, 1H), 6,97 (m, 1H), 6.88 (d, *J* = 7.9 Hz, 1H), 4.95 (s, 2H), 4.06–4.03 (m, 4H), 1.78–1.70 (m, 4H), 1.62–1.58 (m, 2H). ^{13}C-NMR (100 MHz, DMSO-d_6): δ 157.3, 139.2, 138.4, 131.1, 128.1, 127.9, 126.9, 125.1, 123.1, 118.2, 109.2, 58.4, 43.3, 26.6, 23.9. Isomer *E*: ^{1}H-NMR (400 MHz, DMSO-d_6): δ 7.31 (m, 7H), 7.09 (cd, *J* = 7.8, 1.2 Hz, 1H), 6,97 (m, 1H), 4.95 (s, 2H), 3.31 (d, *J* = 5.7 Hz, 4H), 1.78–1.70 (m, 4H), 1.62–1.58 (m, 2H). ^{13}C-NMR (100 MHz, DMSO-d_6): δ 164.6, 143.7, 137.2, 129.8, 129.6, 129.3, 125.7, 125.5, 122.2, 115.8, 110.2, 56.7, 43.2, 25.7, 23.8. MS (ESI+): *m/z* 320 [M+H]. Anal. $C_{20}H_{21}N_3O$ (C, H, N, O).

(*E/Z*)-1-Methyl-3-(morpholinoimino)indolin-2-one (26): Reagents: (*E,Z*)-3-(morpholinoimino)indolin-2-one (168 mg, 0.7 mmol), dimethyl sulfate (92 mg, 0.7 mmol), KOH (51 mg, 0.9 mmol), ethanol (10 mL) and acetone (10 mL). Final product: yellow solid (84.3 mg, 47%), ratio *E*/*Z*: 59:41, m.p: 117–118 °C (lit [40] 116–118 °C).

(*E/Z*)-1-Benzyl-3-(morpholinoimino)indolin-2-ona (27): Reagents: (*E,Z*)-3-(morpholinoimino)indolin-2-one (200 mg, 0.9 mmol), benzyl bromide (148 mg, 0.9 mmol), KOH (63 mg, 1.12 mmol), ethanol (10 mL) and acetone (10 mL). Final product: orange oil (90 mg, 32%), ratio *E*/*Z*: 45:55. Isomer *Z*: ^{1}H-NMR (400 MHz, DMSO-d_6): δ 7.37 (m, 1H), 7.35–7.32 (m, 5H), 7.13 (td, *J* = 7.6, 1.1 Hz, 1H), 6.99 (m, 1H), 6.92 (dt, *J* = 7.9, 0.8 Hz, 1H), 4.95 (s, 2H), 4.01 (m, 4H), 3.82 (m, 4H). ^{13}C-NMR (100 MHz, DMSO-d_6): δ 156.7, 141.1, 139.5, 136.9, 128.7, 127.5, 127.4, 127.3, 123.7, 122.8, 118.3, 108.9, 66.0, 56.9, 42.8. Isomer *E*: ^{1}H-NMR (400 MHz, DMSO-d_6): δ 7.44 (d, *J* = 5.9 Hz, 1H), 7.37 (m, 1H), 7.32 (m, 5H), 7.13 (dt, *J* = 7.6, 1.1 Hz, 1H), 6.99 (m, 1H), 4.95 (s, 2H), 3.82 (m, 4H), 3.28 (m, 4H). ^{13}C-NMR (100 MHz, DMSO-d_6): δ 163.7, 143.9, 141.4, 136.4, 131.5, 128.8, 127.4, 126.2, 125.2, 122.0, 114.8, 109.8, 65.6, 55.3, 42.6. MS (ESI+): *m/z* 322 [M+H]. Anal. $C_{19}H_{19}N_3O_2$ (C, H, N, O).

Synthesis of 28 and 29. The isatin derivative (1 eq) and NaH (1 eq) were dissolved in anhydrous DMF (20 mL), the mixture was stirred at room temperature during 2 h. After that, benzyl bromide (1 eq) was added and stirred until the reaction was finished. The solvent was removed under reduced pressure. Ethyl acetate (50 mL) was added and the organic layer was washed with a satured solution of NaCl (2 × 50 mL). After that, the organic phase was dried over magnesium sulfate and the solvent evaporated under reduced pressure. The crude was purified by column chromatography using chloroform as eluent.

1-Benzylindolin-2,3-dione (28): Reagents: isatin (1 g, 6.8 mmol), benzyl bromide (1.4 g, 8.2 mmol), NaH (196.8 mg, 8.2

mmoL) and DMF (20 mL). Reaction conditions: 1 h at room temperature. Final product: orange solid (1.32 g, 82%), m.p: 132–133 °C (lit. [46] 131–133 °C).

1-Methylindolin-2,3-dione (29): Reagents: isatin (1 g, 6.8 mmol), methyl iodide (1.2 mg, 8.2 mmol), NaH (196.8 mg, 8.2 mmoL) and DMF (20 mL). Reaction conditions: 16 h at room temperature. Final product: orange solid (571.1 g, 52%), m.p: 122–123 °C (lit. [47] 121.7–123.5 °C).

4.2. Molecular modelling

The human LRRK2 sequence was retrieved from Swiss-Prot [48] and aligned to template structure sequence using ClustalW [49]. The percentage of identity between the kinase domain of LRRK2 and the kinase domain of Janus Kinase 2 was 26.3%. Other kinases, for instance TIE2, showed higher percentage of identity. However, they were not used as we could not reproduce with them the same environment around the catalytic residues that has been reported in the literature [24]. Finally, the model using JAK2 as template was built using Swiss-Model [50]. The model has been visualized using Sybyl-X 2.0 [51] showing a RMS value between the model and the 3-D structure of the template of 3.12. Later on, the model was evaluated geometrically using the Ramachandran plot [52] and energetically with the server Verify3D [53]. The docking studies were carried out using the docking program Glide XP implemented in the Schrödinger suite program (Schrödinger, Inc., New York, NY). The inputs complexes to the docking studies were constructed employing the data about the binding site available [24].

4.3. Biology

In vitro LRRK2 and LRRK2 G2019S activity assay. LRRK2 kinase activity was measured using Adapta® Screen technology from Life Technologies™ (Invitrogen) consisting of a fluorescent-based immunoassay for the detection of ADP. Kinase activity was evaluated following the Adapta assay validation protocols PV4873 and PV4881 for LRRK2 and LRRK2 G2019S respectively. Duplicate assay mixtures were set up each in a 10 μL volume containing 17 ng (8 nM) of recombinantly expressed, human LRRK2 protein (Cat. ♯PV4873), 200 μM LRRKtide (Cat. ♯PV5093), 25 mM Tris/7.5 mM HEPES pH 8.2, 5 mM $MgCl_2$, 0.5 mM EGTA, 10 μM ATP, 0.01% NaN_3, 0.005% Brij-35, 1% DMSO and compound of interest in a series of concentrations (e.g. for 10 point titrations, 3-fold serial dilutions are conducted starting from 100 μM concentration) in a 384 well microplate (Corning model 3674). Mutant LRRK2 G2019S inhibition was determined similarly except that due to the higher specific activity 0.5 ng (2.5 nM) of the LRRK2 G2019S mutant kinase (Cat. ♯ PV4881) is used in the assays. A series of controls were incubated on the same plate with: (i) kinase inactivated by EDTA, and (ii) mixtures containing incrementally increased ADP concentrations from 0 to 100 μM, and inversely decreased ATP concentrations from 100 to 0 μM, to establish a standard curve delimited by ADP concentrations corresponding to no conversion and complete conversion of ATP in the assay mixture. After 1 h incubation at ambient temperature, 5 μL of the Adapta® Assay Detection Mix (Cat. ♯ PV5099) was added, containing 30 mM EDTA to stop the kinase reaction, 6 nM of the Eu-labelled anti-ADP antibody (Cat.♯ (PV5097), and 18.9 nM of the AlexaFluor°-ADP conjugate (Cat.♯ PV5098). The plate was allowed to equilibrate at room temperature for at least 30 min before being read out in a fluorescence microplate reader to establish the ratio of emissions at 665 nm (ADP-tracer) and at 615 nm (Eu-antibody) as a measure of ADP concentration by virtue of Fluorescence Resonance Energy Transfer (FRET). The conversion in % of ATP into ADP by the kinase reaction in each well is determined from the ADP/ATP standard curve, and means are formed from each duplicate assay well. The resultant mean conversion ratios for the kinase assays containing increasing concentrations of inhibitor are fitted to a sigmoidal binding model (Graphpad), with the assay containing no inhibitor (<40% ATP conversion for linearity) taken as the 100% activity control (top), and the control assay with the kinase inhibited by excess EDTA as the 0% activity control (bottom). The IC_{50} is determined by the intersection of the fitted curve with the 50% activity measure.

In vitro Parallel artificial membrane permeability assay (PAMPA)-Blood brain barrier (BBB). Prediction of the brain penetration was evaluated using a parallel artificial membrane permeability assay (PAMPA). Ten commercial drugs, phosphate buffer saline solution at pH 7.4 (PBS), ethanol and dodecane were purchased from Sigma, Acros organics, Merck, Aldrich and Fluka. The porcine polar brain lipid (PBL) (catalog no. 141101) was from Avanti Polar Lipids. The donor plate was a 96-well filtrate plate (Multiscreen® IP Sterile Plate PDVF membrane, pore size is 0.45 μM, catalog no. MAIPS4510) and the acceptor plate was an indented 96-well plate (Multiscreen®, catalog no. MAMCS9610) both from Millipore. Filter PDVF membrane units (diameter 30 mm, pore size 0.45 μm) from Symta were used to filter the samples. A 96-well plate UV reader (Thermoscientific, Multiskan spectrum) was used for the UV measurements. Test compounds [(3–5 mg of caffeine, enoxacine, hydrocortisone, desipramine, ofloxacine, piroxicam, testosterone), 12 mg of promazine and 25 mg of verapamile and atenolol] were dissolved in EtOH (1000 μL). 100 μL of this compound stock solution was taken and 1400 μL of EtOH and 3500 μL of PBS pH = 7.4 buffer were added to reach 30% of EtOH concentration in the experiment. These solutions were filtered. The acceptor 96-well microplate was filled with 180 μL of PBS/EtOH (70/30). The donor 96-well plate was coated with 4 μL of porcine brain lipid in dodecane (20 mg mL-1) and after 5 min, 180 μL of each compound solution was added. 1–2 mg of every compound to be determined their ability to pass the brain barrier were dissolved in 1500 μL of EtOH and 3500 μL of PBS pH = 7.4 buffer, filtered and then added to the donor 96-well plate. Then the donor plate was carefully put on the acceptor plate to form a "sandwich", which was left undisturbed for 2 h and 30 min at 25 °C. During this time the compounds diffused from the donor plate through the brain lipid membrane into the acceptor plate. After incubation, the donor plate was removed. UV plate reader determined the concentration of compounds and commercial drugs in the acceptor and the donor wells. Every sample was analyzed at three to five wavelengths, in 3 wells and in two independent runs. Results are given as the mean [standard deviation (SD)] and the average of the two runs is reported. 10 quality control compounds (previously mentioned) of known BBB permeability were included in each experiment to validate the analysis set.

Neurosphere cultures. Proliferation and differentiation assays. All animal care and handling was carried out in accordance with European Union guidelines (directives 86/609/EEC and 2010/63/EU) and Spanish legislation (Law 32/2007 and RD 53/2013), and the protocols were approved by the Ethical Committee of the Consejo Superior de Investigaciones Cientificas (CSIC) and Comunidad de Madrid. All efforts were made to ameliorate the suffering of the animals and to reduce the number of animals used to a minimum.

Neurosphere (NS) cultures were derived from the subventricular zone of 4 young adult (6 weeks old) C57BL/6 mice and induced to proliferate using established passaging methods to achieve optimal cellular expansion according to published protocols [54]. Briefly, mice were euthanized with CO_2, brains were removed and the subventricular zone was dissected, cut up into pieces and digested using 0.7 mg/ml papain, 0.2 mg/ml cysteine and 0.2 mg/ml EDTA before it was gently disaggregated. The resulted cell suspension was plated into 8 wells of 12-well plates

containing DMEM-F12 supplemented with insulin (10 mg/ml), apotransferrin, putrescine, progesterone, sodium selenite (N2), and B27. The cells were passaged by mechanical procedures and were maintained until passaged 3 for the first experiments, with alternative daily addition of both 10 ng/ml of fibroblast growth factor (FGF, Peprotech Cat No. 100-18B) and 2 ng/mL of epidermal growth factor (EGF, Peprotech Cat No. AF-100-15). Cell proliferation assays were performed on floating neurospheres in 96-well plates at a density of 5000 cells/cm^2. LRRK2 inhibitors were diluted in DMSO at a concentration of 10 mM and then added to the dissociated cells to a final concentration of 5 μM and 0.1% DMSO was used as a control. Each treatment was repeated by triplicate and the cells were left to grow at 37 °C and 5% of CO_2 in an incubator for 3 days. On the third day, for the measurement of the size and number of the neurospheres, photographs were taken by bright field microscopy using an automatic platten, taken 6 pictures of different areas of each well with the 10X objective. The total number and area of neurospheres bigger than 400 μm [2] cell area was measured using a macro software for Image J, (NIH, Bethesda, MD) designed at the Cajal Institute. Quantitative analyses were carried out in three separate experiments, calculating the mean ± SEM and using a two-tailed Student's *t*-test to determine statistically relevant changes.

Acknowledgements

Financial support from MINECO (grant no. SAF2012-37979-C03-01 and RTC-2015-3439-1 to A. M. and BFU2014-57494-R to A. V. M), MECD (FPU13-003262 to J. Z. D.). Technical assistance of Maria Ciorraga is also acknowledged. A.M. and C.G are members of the "CIB Intramural Program "Molecular Machines for Better Life" (MACBET)"

Appendix A. Supplementary data

Supplementary data related to this article can be found at http://dx.doi.org/10.1016/j.ejmech.2017.06.060.

References

[1] A. Zimprich, S. Biskup, P. Leitner, P. Lichtner, M. Farrer, S. Lincoln, J. Kachergus, M. Hulihan, R.J. Uitti, D.B. Calne, A.J. Stoessl, R.F. Pfeiffer, N. Patenge, I.C. Carbajal, P. Vieregge, F. Asmus, B. Muller-Myhsok, D.W. Dickson, T. Meitinger, T.M. Strom, Z.K. Wszolek, T. Gasser, Mutations in LRRK2 cause autosomal-dominant parkinsonism with pleomorphic pathology, Neuron 44 (2004) 601–607.
[2] D.G. Healy, M. Falchi, S.S. O'Sullivan, V. Bonifati, A. Durr, S. Bressman, A. Brice, J. Aasly, C.P. Zabetian, S. Goldwurm, J.J. Ferreira, E. Tolosa, D.M. Kay, C. Klein, D.R. Williams, C. Marras, A.E. Lang, Z.K. Wszolek, J. Berciano, A.H. Schapira, T. Lynch, K.P. Bhatia, T. Gasser, A.J. Lees, N.W. Wood, L.C. International, Phenotype, genotype, and worldwide genetic penetrance of LRRK2-associated Parkinson's disease: a case-control study, Lancet Neurol. 7 (2008) 583–590.
[3] P.J. Gilligan, Inhibitors of leucine-rich repeat kinase 2 (LRRK2): progress and promise for the treatment of Parkinson's disease, Curr. Top. Med. Chem. 15 (2015) 927–938.
[4] A.A. Estrada, Z.K. Sweeney, Chemical biology of leucine-rich repeat kinase 2 (LRRK2) inhibitors, J. Med. Chem. 58 (2015) 6733–6746.
[5] M.R. Cookson, LRRK2 pathways leading to neurodegeneration, Curr. Neurol. Neurosci. Rep. 15 (2015) 42.
[6] M. Steger, F. Tonelli, G. Ito, P. Davies, M. Trost, M. Vetter, S. Wachter, E. Lorentzen, G. Duddy, S. Wilson, M.A. Baptista, B.K. Fiske, M.J. Fell, J.A. Morrow, A.D. Reith, D.R. Alessi, M. Mann, Phosphoproteomics reveals that Parkinson's disease kinase LRRK2 regulates a subset of Rab GTPases, Elife 5 (2016).
[7] J.Q. Li, L. Tan, J.T. Yu, The role of the LRRK2 gene in Parkinsonism, Mol. Neurodegener. 9 (2014) 47.
[8] D.C. Berwick, K. Harvey, LRRK2: an eminence grise of Wnt-mediated neurogenesis? Front. Cell Neurosci. 7 (2013) 82.
[9] A. Abdipranoto, S. Wu, S. Stayte, B. Vissel, The role of neurogenesis in neurodegenerative diseases and its implications for therapeutic development, CNS Neurol. Disord. Drug Targets 7 (2008) 187–210.
[10] O. Lamm, J. Ganz, E. Melamed, D. Offen, Harnessing neurogenesis for the possible treatment of Parkinson's disease, J. Comp. Neurol. 522 (2014) 2817–2830.
[11] Y. Hirota, M. Sawada, S.H. Huang, T. Ogino, S. Ohata, A. Kubo, K. Sawamoto, Roles of Wnt signaling in the neurogenic niche of the adult mouse ventricular-subventricular zone, Neurochem. Res. 41 (2016) 222–230.
[12] S. Wetzel, R.S. Bon, K. Kumar, H. Waldmann, Biology-oriented synthesis, Angew. Chem. Int. Ed. Engl. 50 (2011) 10800–10826.
[13] W. Wilk, T.J. Zimmermann, M. Kaiser, H. Waldmann, Principles, implementation, and application of biology-oriented synthesis (BIOS), Biol. Chem. 391 (2010) 491–497.
[14] A. Medvedev, O. Buneeva, V. Glover, Biological targets for isatin and its analogues: implications for therapy, Biologics 1 (2007) 151–162.
[15] M. Kaur, M. Singh, N. Chadha, O. Silakari, Oxindole: a chemical prism carrying plethora of therapeutic benefits, Eur. J. Med. Chem. 123 (2016) 858–894.
[16] A.A. Ikotun, G.O. Egharevba, C.A. Obafemi, A.O. Owoseni, Ring deactivating effect on antimicrobial activities of metal complexes of the schiff base of p-nitroaniline and isatin, J. Chem. Pharm. Res. 4 (2012) 416–422.
[17] M. Pandey, D.S. Raghuvanshi, K.N. Singh, Microwave-assisted, solvent-free synthesis of 3'-(aryl/heteroaryl)-1-morpholinomethyl/piperidinomethylspiro [3H-indole-3,2'-thiazolidine]-2,4'(1H)-diones via 3-isatinimines, J. Heterocycl. Chem. 46 (2009) 49–53.
[18] N. Kaur, D. Kishore, Montmorillonite: an efficient, heterogeneous and green catalyst for organic synthesis, J. Chem. Pharm. Res. 4 (2012) 991–1015.
[19] O. Ottoni, R. Cruz, R. Alves, Efficient and simple methods for the introduction of the sulfonyl, acyl and alkyl protecting groups on the nitrogen of indole and its derivatives, Tetrahedron 54 (1998) 13915–13928.
[20] L. Correia Guedes, J.J. Ferreira, M.M. Rosa, M. Coelho, V. Bonifati, C. Sampaio, Worldwide frequency of G2019S LRRK2 mutation in Parkinson's disease: a systematic review, Park. Relat. Disord. 16 (2010) 237–242.
[21] A.B. West, D.J. Moore, S. Biskup, A. Bugayenko, W.W. Smith, C.A. Ross, V.L. Dawson, T.M. Dawson, Parkinson's disease-associated mutations in leucine-rich repeat kinase 2 augment kinase activity, Proc. Natl. Acad. Sci. U. S. A. 102 (2005) 16842–16847.
[22] M. Liu, S.A. Bender, G.D. Cuny, W. Sherman, M. Glicksman, S.S. Ray, Type II kinase inhibitors show an unexpected inhibition mode against Parkinson's disease-linked LRRK2 mutant G2019S, Biochemistry 52 (2013) 1725–1736.
[23] M. Hassanein, M.H. Almahayni, S.O. Ahmed, S. Gaballa, R. El Fakih, FLT3 inhibitors for treating acute myeloid leukemia, Clin. Lymphoma Myeloma Leuk. 16 (2016) 543–549.
[24] H. Chen, B.K. Chan, J. Drummond, A.A. Estrada, J. Gunzner-Toste, X. Liu, Y. Liu, J. Moffat, D. Shore, Z.K. Sweeney, T. Tran, S. Wang, G. Zhao, H. Zhu, D.J. Burdick, Discovery of selective LRRK2 inhibitors guided by computational analysis and molecular modeling, J. Med. Chem. 55 (2012) 5536–5545.
[25] L. Di, E.H. Kerns, K. Fan, O.J. McConnell, G.T. Carter, High throughput artificial membrane permeability assay for blood-brain barrier, Eur. J. Med. Chem. 38 (2003) 223–232.
[26] P. Crivori, G. Cruciani, P.A. Carrupt, B. Testa, Predicting blood-brain barrier permeation from three-dimensional molecular structure, J. Med. Chem. 43 (2000) 2204–2216.
[27] A. Ernst, K. Alkass, S. Bernard, M. Salehpour, S. Perl, J. Tisdale, G. Possnert, H. Druid, J. Frisen, Neurogenesis in the striatum of the adult human brain, Cell 156 (2014) 1072–1083.
[28] S. Gil-Perotin, M. Duran-Moreno, A. Cebrian-Silla, M. Ramirez, P. Garcia-Belda, J.M. Garcia-Verdugo, Adult neural stem cells from the subventricular zone: a review of the neurosphere assay, Anat. Rec. Hob. 296 (2013) 1435–1452.
[29] C. Herrera-Arozamena, O. Marti-Mari, M. Estrada, M. de la Fuente Revenga, M.I. Rodriguez-Franco, Recent advances in neurogenic small molecules as innovative treatments for neurodegenerative diseases, Molecules 21 (2016), http://dx.doi.org/10.3390/molecules21091165.
[30] A. Kriza, I. Ignat, N. Stanica, C. Draghici, Synthesis and characterization of Cu(II), Co(II) and Ni(II) complexes with Schiff bases derived from isatin, Rev. Chim. 62 (2011) 696–701.
[31] K.L. Vine, J.M. Locke, M. Ranson, K. Benkendorff, S.G. Pyne, J.B. Bremner, In vitro cytotoxicity evaluation of some substituted isatin derivatives, Bioorg. Med. Chem. 15 (2007) 931–938.
[32] V.V. Kouznetsov, J.S. Bello, D.F. Amado, A simple entry to novel spiro dihydroquinoline-oxindoles using Povarov reaction between 3-N-arylimi-noisatins and isoeugenol, Tetrahedron Lett. 49 (2008) 5855–5857.
[33] A. Dandia, M. Saha, A. Shivpuri, Improved synthesis of trifluoromethyl substituted 3-spiro indolines and 3-indolyimines under microwaves irradiation, Indian J. Chem. Technol. 4 (1997) 201–205.
[34] K.M. Khan, U.R. Mughal, P.,S. Samreen, M.I. Choudhary, Schiff bases of isatin: potential anti-leishmanial agents, Lett. Drug Des. Discov. 5 (2008) 243–249.
[35] J.Y. Ma, Y.C. Quan, H.G. Jin, X.H. Zhen, X.W. Zhang, L.P. Guan, Practical synthesis, antidepressant, and anticonvulsant activity of 3-phenyliminoindolin-2-one derivatives, Chem. Biol. Drug Des. 87 (2016) 342–351.
[36] S.B. Bari, A.O. Agrawal, U.K. Patil, Synthesis and pharmacological evaluation of some novel isatin derivatives for antimicrobial activity, J. Sci. Islam. Repub. Iran. 19 (2008) 217–222.
[37] G.M. Šekularac, J.B. Nikolić, P.B.,B. Petrović, B. Đurovićsaša, Z. Drmanić, Synthesis, antimicrobial and antioxidative activity of some new isatin derivatives, J. Serb. Chem. Soc. 79 (2014) 1347–1354.
[38] A. McGookin, Reactive methylene groups. III. The ehrlich-sachs reaction, J. Appl. Chem. 5 (1955) 65–66.
[39] J. Azizian, A.V. Morady, S. Soozangarzadeh, A. Asadi, Synthesis of novel spiro-[3H-indole-3,3'-[1,2,4]triazolidine]-2-ones via azomethine imines, Tetrahedron Lett. 43 (2002) 9721–9723.

[40] F.D. Popp, Potential anticonvulsants. IX. Some isatin hydrazones and related compounds, J. Heterocycl. Chem. 21 (1984) 1641–1645.
[41] Y.M.S.A. Al-Kahraman, G.S. Singh, M. Yasinzai, Evaluation of N-(2-thienylidene)amines, N-(2-hydroxybenzylidene)amines and 3-iminoindolin-2-ones as antileishmanial agents, Lett. Drug Des. Discov. 8 (2011) 491–495.
[42] B. Zhang, P. Feng, L.H. Sun, Y. Cui, S. Ye, N. Jiao, N-Heterocyclic carbene-catalyzed homoenolate additions with N-aryl ketimines as electrophiles: efficient synthesis of spirocyclic γ-lactam oxindoles, Chem. Eur. J. 18 (2012) 9198–9203.
[43] G. Bianchini, P. Ribelles, D.;T.,R.M. Becerra, J.C. Menéndez, Efficient synthesis of 2-acylquinolines based on an aza-vinylogous Povarov reaction, Org. Chem. Front. 3 (2016) 412–422.
[44] G.S. Singh, N. Siddiqui, S.N. Pandeya, Synthesis and anticonvulsant and anti-inflammatory activities of new 3-aryl/alkylimino-1-methylindol-2-ones, Arch. Pharm. Res. 15 (1992) 272–274.
[45] A. Corsico Coda, G. Desimoni, A. Gamba Invernizzi, P. Quadrelli, P.P.;G.,T. Righetti, Copper(II) in organic synthesis. VI1 reaction of the copper(II) acetate complex of 1-methylisatin-3-chlorophenylhydrazone with dimethyl acetylenedicarboxylate, Tetrahedron 43 (1987) 2843–2852.
[46] S. Sarel, J.T. Klug, Synthesis and properties of 2,2-diphenylindoxyl, Isr. J. Chem. 2 (1964) 143–150.
[47] C. Zhang, S. Li, F. Bureš, R. Lee, X. Ye, Z. Jiang, Visible light photocatalytic aerobic oxygenation of indoles and pH as a chemoselective switch, ACS Catal. 6 (2016) 6853–6860.
[48] A. Bairoch, B. Boeckmann, S. Ferro, E. Gasteiger, Swiss-Prot: juggling between evolution and stability, Brief. Bioinform. 5 (2004) 39–55.
[49] J.D. Thompson, D.G. Higgins, T.J. Gibson, CLUSTAL W: improving the sensitivity of progressive multiple sequence alignment through sequence weighting, position-specific gap penalties and weight matrix choice, Nucleic Acids Res. 22 (1994) 4673–4680.
[50] N. Guex, M.C. Peitsch, SWISS-MODEL and the Swiss-PdbViewer: an environment for comparative protein modeling, Electrophoresis 18 (1997) 2714–2723.
[51] A. Ghose, E. Jaeger, P. Kowalczyk, M. Peterson, A. Treasurywala, Conformational searching methods for small molecules. I. Study of the SYBYL SEARCH method, J. Comp. Chem. 14 (1993) 1050–1065.
[52] K. Gopalakrishnan, G. Sowmiya, S.S. Sheik, K. Sekar, Ramachandran plot on the web (2.0), Protein Pept. Lett. 14 (2007) 669–671.
[53] D. Eisenberg, R. Luthy, J.U. Bowie, VERIFY3D: assessment of protein models with three-dimensional profiles, Methods Enzymol. 277 (1997) 396–404.
[54] V. Nieto-Estevez, C.O. Oueslati-Morales, L. Li, J. Pickel, A.V. Morales, C. Vicario-Abejon, Brain insulin-like growth factor-I directs the transition from stem cells to mature neurons during postnatal/adult hippocampal neurogenesis, Stem Cells 34 (2016) 2194–2209.